ORGANIC ELECTRODE MATERIALS FOR ELECTRICAL ENERGY STORAGE DEVICES

A Dissertation

Presented to the Faculty of the Graduate School

of Cornell University

In Partial Fulfillment of the Requirements for the Degree of

Doctor of Philosophy

by

Sean Conte

August 2013

ORGANIC ELECTRODE MATERIALS FOR ELECTRICAL ENERGY STORAGE DEVICES

Sean Conte, Ph.D.

Cornell University 2013

In order to develop next generation cathode materials for electrical energy storage (EES) devices, this study has focused on synthesis and electrochemical characterization of redox-active organic materials. Organic molecules are composed of widely-available, lightweight elements, and its properties can be rationally tuned using well-known principles of organic chemistry. Moreover, both amorphous and crystalline organic materials can accommodate more dramatic changes in volume than the inorganic systems currently being proposed for next-generation lithium batteries. Discrete organic compounds are inadequate on its own: the high solubility in electrolyte media results to a rapid fade in the capacity and organic materials are usually insulators. In order for these materials to be of practical use, it was crucial to develop methodologies and new materials by which these species can be confined to an insoluble conductive substrate without altering their electrochemical properties.

BIOGRAPHICAL SKETCH

Sean Conte was born in a town right outside of Tokyo, Japan. He graduated from Quince Orchard High School in Maryland and earned his bachelor's degree from Pennsylvania State University in Chemistry with Mathematics as a minor. In his time at Penn State, he was fortunate to work in Professor Mark Maroncelli's lab performing computational studies of ionic liquid. After graduating college, he briefly worked in Maryland purifying proteins until he decided to leave the company to pursue a PhD in Chemistry at Cornell University, joining Professor Héctor Abruña's lab to work on organic-based electrode materials.

This dissertation is dedicated to my dear mother and brother for their endless love, support, and encouragement.

ACKNOWLEDGMENTS

I would like to sincerely and gratefully thank Professor Héctor Abruña for his guidance, patience, and understanding throughout my graduate studies at Cornell University. I am also grateful to the other members of my PhD committee, Professors Francis DiSalvo and William Dichtel, and the Chemistry Department for their helpful suggestions.

I will always be thankful to my former college research advisor, Professor Mark Maroncelli. I still remember fondly of my time working in his lab. His influence was the main reason for my decision to pursue a PhD in Chemistry.

A good support system is vital for surviving graduate school. I would like to thank the friendship I formed with Dr. Coalton Bennett "Third Eye Vision". I will truly miss our 'cLaaaaazy' conversations we had. Thanks for introducing me to the world of Jungle and Drum & Bass. Dr. Joshua Parks "PL", you have been an awesome friend to me. I will always remember our robot RIN-G3. The new model RIN-G∞ will be arriving in San Francisco soon, so please embrace yourself! Dr. Cen (Joanna) Tan "JB", you were someone that I shared the good and the bad times in Cornell. I will always remember our 'Asian Philosophies' that we shared and your catch-phrase "Grrrrrr!". My two favorite PRz, Gabriel Rodriguez-Calero and Kenneth Hernandez-Burgos, thanks for making my time in the lab very enjoyable. May the 'SITUATION' be with you. I would also like to thank the other past and present Abruñies: Jimmy John, Dr. Jie Gao, Dr. Michael Lowe, Dr. Stephen Burkhardt, Dr. Yu-Wu Zhong, Dr. Hualei Qian, Dr. Weidong Zhou, Dr. David Finkelstein, and Dr. Michele Tague.

Finally, and most importantly, I would like to thank my family and my girlfriend for their support, encouragement, patience, and unwavering love.

TABLE OF CONTENTS

BIOGRAPHICAL SKETCH iii

DEDICATION iv

ACKNOWLEDGEMENTS v

TABLE OF CONTENTS vi

LIST OF FIGURES ix

LIST OF SCHEMES. xii

LIST OF TABLES xiii

CHAPTER ONE:
ELECTROACTIVE ORGANIC MATERIALS FOR ELECTRICAL ENERGY STORAGE DEVICES

1-1. Introduction – Organic Electrode Materials 1

1-2. Electrical Energy Storage Devices: Batteries & Capacitors 1

1-3. Electroactive Organic Groups 6

1-4. Addressing the Shortcomings of Organics – ‘Hybrid’ Approach 10

1-5. Dissertation Overviews 11

1-6. References 14

CHAPTER TWO:
EXPERIMENTAL

2-1. Reagents and Materials 18

2-2. Electrochemical Measurements. 19

2-3. Device Testings. 20

2-4. Computational Methods 20

2-5. Synthesis. 20

2-6. References. 32

CHAPTER THREE:
INVESTIGATION OF NEW THIOETHER-BASED THIOPHENES FOR PSEUDOCAPACITIVE ELECTRODES

3-1. Introduction. 35

3-2. Synthesis 37

3-3. Redox Behavior. 38

3-4. Summary & Conclusions. 43

3-5. References. 44

CHAPTER FOUR:
DESIGNING CONDUCTING POLYMER FILMS FOR ELECTROCHEMICAL ENERGY STORAGE TECHNOLOGIES

4-1. Introduction. 46

4.2. Synthesis Pathway and Design Criteria 48

4-3. Cyclic Voltammetry Experiments of Monomers in Solution. 49

4-4. Electrochemistry of Electroactive Films 53

4-5. Computational Studies. 56

4-6. Conclusions 59

4-7. References 59

CHAPTER FIVE:
ELECTROCHEMICAL CHARACTERIZATION & DEVICE TESTING OF POLY-(EDOT-TAPD) FILM

5-1. Introduction 62

5-2. Electrochemical Study – Solvent Dependence 65

5-3. Sample Preparation and Device Testing 68

5-4. Summary & Conclusions. 70

5-5. Comments on ‘Hybrid’ Materials 71

5-6. References. 73

CHAPTER SIX:
POST-POLYMERIZATION MODIFICATION AS A METHOD FOR GENERATING ELECTROACTIVE HYBRID-POLYMER

6-1. Introduction. 74

6-2. Synthesis of Poly-(EDOT-DMcT) 76

6-3. Electrochemical Characterization & Cyclability. 78

6-4. Summary & Conclusions. 79

6-5. References 80

CHAPTER SEVEN:
FUTURE DIRECTIONS

7-1. Future Research Directions 82

7-2. Electropolymerization of Non-Conductive Redox Polymers 82

7-3. Symmetric EES Devices 84

7-4. Anchoring Electroactive Compounds on Other Insoluble Substrates . 85

7-5. References 86

LIST OF FIGURES

Figure 1-1. EES devices with corresponding discharge curves. 2

Figure 1-2. Ragone plot for various energy storage and generation systems 3

Figure 1-3. Redox property of organic disulfide 6

Figure 1-4. Redox property of violene, BMTbT 7

Figure 1-5. Redox property of nitroxide 8

Figure 1-6. Redox property of carbonyl 9

Figure 1-7. Redox property of conducting polymer 10

Figure 1-8. Schematic depiction of the 'hybrid' approach 11

Figure 1-9. 2,5-Bis(methylthio)thieno[3,2-*b*]thiophene **(**FBMTbT). 12

Figure 1-10. Redox property of poly-(EDOT-TAPD). 13

Figure 1-11. Post-polymerization reaction: DMcT confinement on PEDOT 14

Figure 3-1. 5,5'-Bis(methylthio)-2,2'-bithiophene (BMTbT) **1** 36

Figure 3-2. New thiophene derivatives for potential cathode materials 37

Figure 3-3. CV of 5mM **3** and 0.1M TBAH in AN, 100 mV/s 38

Figure 3-4. Redox properties of hexaazaoctadecahydrocoronene and **3** 40

Figure 3-5. CV of 0.2mM **4** in 0.1M TBAH/AN, 20 mV/s. 40

Figure 3-6. (a) RDE of 1mM **4** in 0.1M TBAH/AN at 10 mV/s, inset contains a Levich plot at 0.7 V (b) Koutecky-Levich plot at 0.62V 42

Figure 4-1. Chemical structures of the hybrid electro-active monomer. (**5**) N,N,N',N'- Tetramethyl-*p*-phenyldiamine (TMPD), (**6**) 1-(4-dimethylamino)pyrrole, (**7**) *N*-(2-(1*H*-pyrrol-1-yl)ethyl)-*N*-ethyl-*N',N'*-dimethyl-*p*-phenylenediamine, (**8)** *N*-((2,3-dihydrothieno[3,4-b][1,4]dioxin-2-yl)methyl)-*N',N'*-dimethyl-*p*-phenylenediamine, (**9**) *N*-((2,3-dihydrothieno[3,4-b][1,4]dioxin-2-yl)methyl)-*N*-ethyl-*N*',*N*'-dimethyl-*p*-phenylenediamine 47

Figure 4-2. Representative CVs (first cycles) of monomers **5** (10 mM), **6** (10 mM), **7** (10 mM), and **8** (10 mM) in 0.1 M TBAP/AN solutions at a sweep rate of 20 mV/s 50

Figure 4-3. Representative CV of the electropolymerization of 20 mM monomer **9** in 0.1 M TBAP/AN at a sweep rate of 20 mV/s 52

Figure 4-4. Representative CV of the first two cycles for the CP film-modified GCEs of (a) poly-**9**, and (b) poly-**8** at a sweep rate of 20 mV/s. 53

Figure 4-5. (a) Sweep rate dependent CVs and (b) Peak current vs sweep rate plot for a polymer **9** film-modified GCE 54

Figure 4-6. (a) Electrochemical cycling of polymer **9** film-modified GCE at 500 mV/s, and (b) normalized peak current vs. number of cycles. . . 56

Figure 4-7. Calculated oxidation potentials for **6**-**9** vs. the observed first oxidation. The high correlation suggests that the ground state properties of both neutral and oxidized forms are well described at this level of theory 57

Figure 4-8. SOMO and SOMO-1 eigenvalues and isosurfaces for **6**-**9**. Isosurfaces are in agreement with the assumptions for film preparation (that the third oxidation leads to film formation). SOMO and SOMO-1 levels also suggest that **6** will be difficult to polymerize due to very positive oxidations. 57

Figure 5-1. Schematic depiction of the ‘hybrid’ approach. 62

Figure 5-2. Redox property of poly-**9**. 63

Figure 5-3. Co-electropolymerization of pyrrole and ferrocene-functionalized pyrrole 64

Figure 5-4. Film electrochemistry of poly-**9** in different solvents 67

Figure 5-5. SEM image of poly-**9**. 68

Figure 5-6. Charge-discharge curves of (a) poly-**9** and (b) PEDOT at 1C. 69

Figure 5-7. Polymerization of Thiophene-Tetrathiafulvalene monomer utilizing Yamamoto coupling. 71

Figure 5-8. New synthesis scheme for TAPD ‘hybrid’ polymers 72

Figure 6-1. Redox property of 2,5-dimercapto-1,3,4-thiadiazole (DMcT) 74

Figure 6-2. Electropolymerization of EDOT-OTs **11**. 77

Figure 6-3. Reaction progress of **11** with dilithiated DMcT **12** 77

Figure 6-4. Scan rate dependence of **13** 78

Figure 6-5. Cyclability performance of **13** 79

Figure 7-1. Electropolymerization of non-conductive redox polymers on carbon. 83

Figure 7-2. Symmetric EES electrode monomers and its polymeric form. 84

Figure 7-3. CV of 3mM of acetyl-DMPD in 0.1M TBAP/AN. 85

Figure 7-4. CV of DMPD-carbon composite and the plot of i_{pc} vs scan rate. . . . 86

LIST OF SCHEMES

Scheme 3-1. Synthesis scheme of **2**, **3** and **4** 38

Scheme 4-1. Synthesis scheme of hybrid monomers **6**, **7**, **8**, and **9** 48

Scheme 6-1. Synthesis scheme of **10** and its electropolymerization 75

Scheme 6-2. Synthesis scheme of ‘hybrid’ polymer **13** 76

LIST OF TABLES

Table 1-1. LIB cathodes and properties 5

Table 3-1. Cathode materials and properties 43

Table 4-1. Electrochemical parameters and its values for the molecules under study 49

Table 5-1. Dielectric constants and percent film deterioration in different solvents 65

CHAPTER ONE

ELECTROACTIVE ORGANIC MATERIALS FOR ELECTRICAL ENERGY STORAGE DEVICES

1-1 Introduction – Organic Electrode Materials

Electroactive organic materials are one of the leading thrusts for replacing traditional inorganic electrodes for today's emerging market needs as they present attractive opportunities for technological advancement in the field of battery and capacitive storage science technologies. Organic compounds exhibit new possibilities for high energy/power density devices, cost-effectiveness, and environmental consciousness delivering highly engineerable options in tunability, abundancy, and sustainability.[1-4] Organics were not considered as an important class of electrode materials for a long time because inorganic materials have enjoyed larger success and more rapid development. Furthermore, the slow development of conducting polymers as rechargeable cathodes also contributed to the lack of attention in organic electrodes since the late 1980's.[5] However, the concept of using organics as electrode materials is as seasoned as inorganic counterpart. For example, the first commercialized primary lithium battery implemented the use of organics with a $(CF)_n$-Li configuration.[6] Now that intercalation materials have reached their intrinsic limits, a renewed interest on organic electrodes is witnessed with the explosion of literature on this topic in the recent years.

1-2 Electrical Energy Storage Devices: Batteries & Capacitors

The two primary electrical energy storage (EES) devices are batteries and capacitors.[7] Even though both rely on electrochemical processes, the respective properties

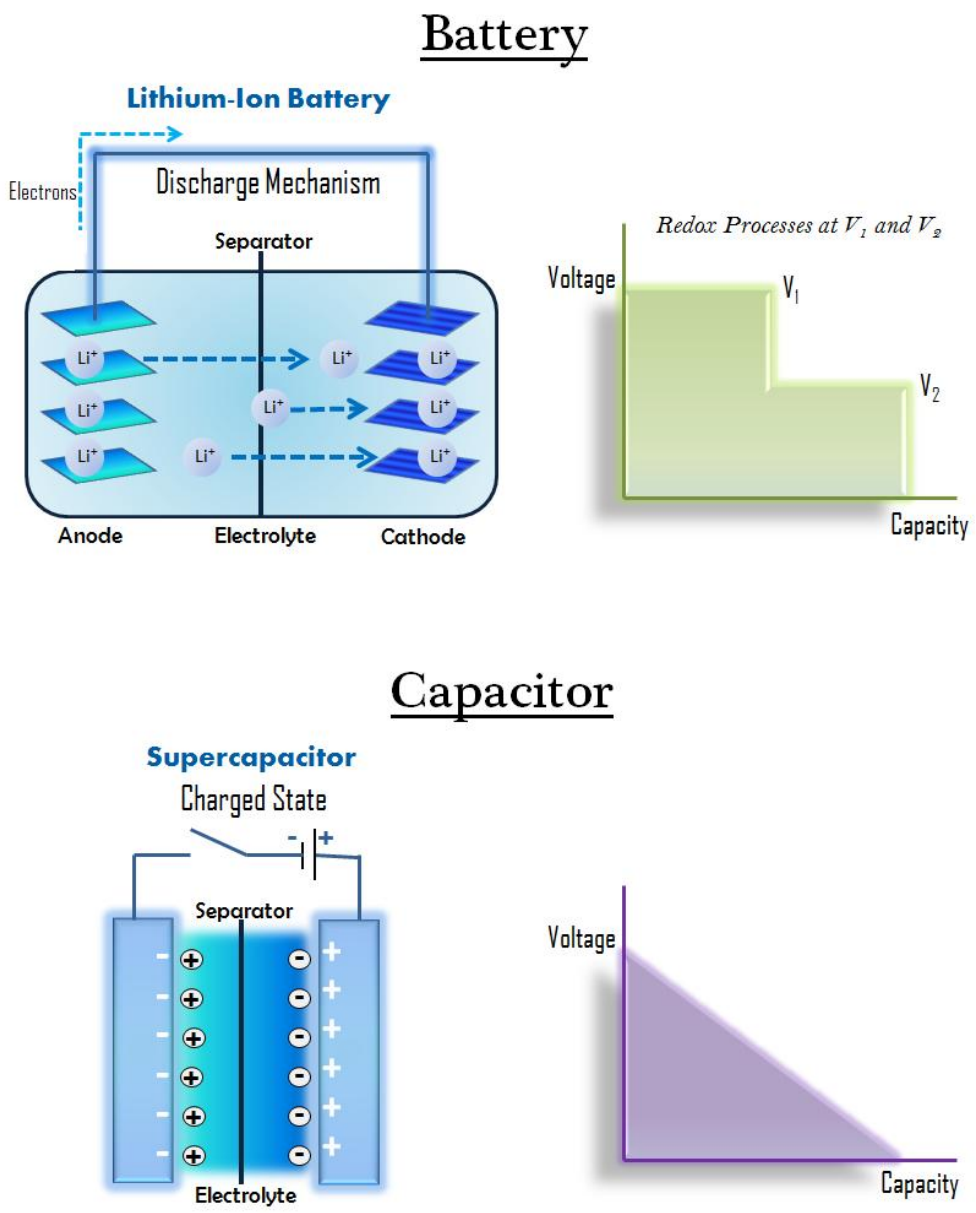

Figure 1-1. EES devices with corresponding discharge curves.

are fundamentally different due to their different mechanism of charge and energy storage: batteries store energy from chemical reactions, while capacitors store energy through physical charges. Figure 1-1 depicts a representative figure of each type of device and the corresponding characteristic discharge curves (voltage vs. capacity). Capacitors show a downwards sloping trend in the discharge curve, while batteries show

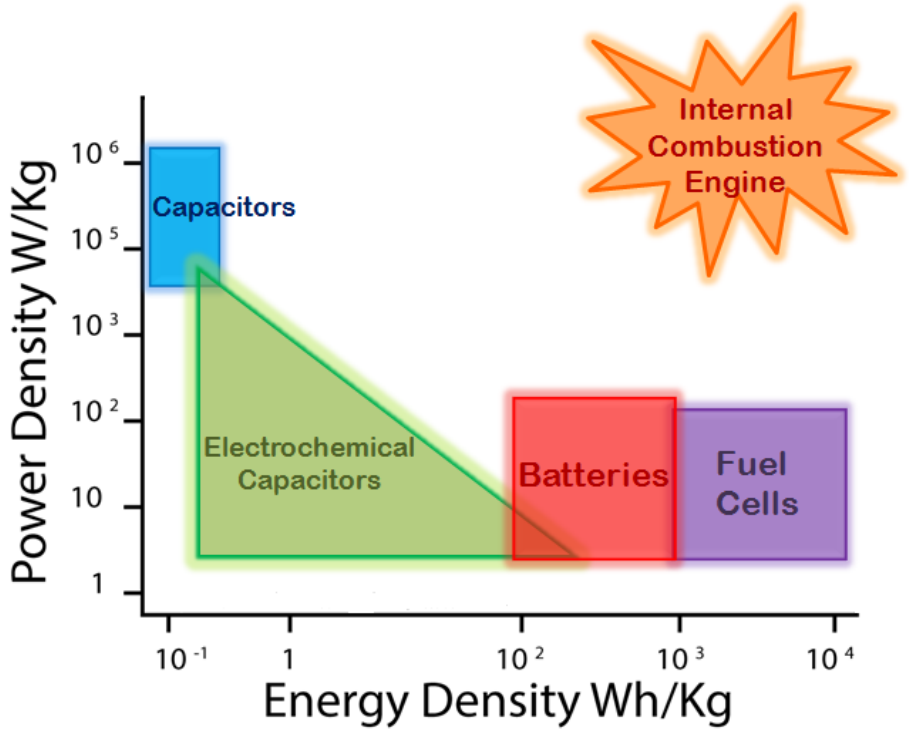

Figure 1-2. Ragone plot for various energy storage and generation systems.[9]

plateaus depending on the number of redox processes involved.[8] The Ragone plot (Figure 1-2), which illustrates the relationship between energy and power densities of different energy storage and generation devices, summarizes the different nature of these two EES devices.[9] Batteries possess much higher energy density compared to capacitors, but capacitors offer higher power-output. These differences allow each to be employed in different applications depending on the requirements.

A battery is an electrochemical device that consists of an electropositive material (anode), an electronegative material (cathode), an electrolyte, and a separator that electrically isolates the two electrodes (Figure 1-1). The chemical energy is converted to electrical energy by utilizing the redox reactions (faradaic processes) at each electrode. The overall performance of a battery is not limited to the chemical and physical processes that occur at and between the electrodes, but also the interactions with the electrolyte

solution (solvent & ions). Electrochemical techniques such as cyclic voltammetry offer a reliable and a quick analysis of the redox properties and stability/performance in many different solvents and supporting electrolytes.

Batteries are divided into main two categories: primary and secondary. Primary batteries are those that are discarded after completion of a discharge, while secondary batteries are those that can be recharged and used repeatedly. Lead-acid batteries, invented in 1859 by the French physicist Gaston Planté, are the oldest type of rechargeable batteries.[10] The first model employed two lead sheets separated by rubber strips and was rolled into a spiral. Lead-acid batteries were first used to power the lights in train carriages stopping at a station. Because lead-acid and other rechargeable batteries such as the Nickel-Cadmium system utilize highly toxic materials and suffer from low energy densities, new battery technologies have focused mainly on the advancement of lithium-ion technologies. The commercialization of rechargeable lithium-ion batteries (LIB) has germinated a global change in user's daily lives due to the rapid rise of portable technologies. Lithium-based technologies present the highest gravimetric and volumetric energy densities. Quite simply, lithium offers two key advantages: the extreme negative potential of the Li/Li^+ redox couple at -3.05V vs NHE and the low weight of 6.94g/mol.

Lithium, as an anode, can provide an extremely high theoretical capacity (3,860 mAh/g) and high voltage (with the appropriate cathode), but lithium dendrite formation during the deposition of lithium on its surface caused significant safety issues and poor cyclability performance.[11] The practical shortcomings of lithium have been overcome through the utilization of carbon materials at the expense of significantly lowering the

Electrode material	Voltage (V vs Li/Li^+)	Specific capacity (mAh/g)	Specific energy (Wh/kg)
$LiCoO_2$	3.7	140	518
$LiMn_2O_4$	4.0	100	400
$LiNiO_2$	3.5	180	630
$LiFePO_4$	3.3	150	495
Li_2FePO_4F	3.6	115	414
$LiCo_{1/3}Ni_{1/3}Mn_{1/3}O_2$	3.6	160	576
$Li(Li_aNi_xMn_yCo_z)O_2$	4.2	220	920

Table 1-1. LIB cathodes and properties.

anode capacity. For example, graphite (372 mAh/g), exhibits highly reversible lithium intercalation-deintercalation processes taking place at potentials near the lithium redox couple.[12] Today, other materials such as silicon, metal oxides, and lithium alloys are generating enormous interest as LIB anodes with the aim of further enhancing its capability (capacity, cyclability/stability).[13-15] Many intercalation compounds of metal oxides and metal phosphates have been studied as LIB cathode materials, with $LiCoO_2$ being one of the most extensively used in commercial applications. Table 1-1 summarizes the properties (voltages vs Li/Li^+, capacities, and energy densities) of some LIB cathodes.

Like a battery, an electrochemical capacitor (EC) is an electrochemical cell that consists of two electrodes, an electrolyte, and a separator (Figure 1-1). ECs are also known as supercapacitors or ultracapacitors due to the superior capacity compared to conventional dielectric capacitors. The major difference between the two EES devices is the type of charge storage mechanism utilized. As mentioned previously, batteries store energy through chemical reactions and capacitors through physical charges. Electrical

double layer capacitors (EDLC) are ECs that store charges through an electrical double layer (EDL), which is a charge separation formed at the interface between an electrode and an electrolyte solution.[16-20] The absence of chemical or phase changes (no structural changes) can provide high power capability and long-term cyclability. High-surface area carbons such as activated carbon are usually employed as electrodes in EDLCs. ECs that utilize faradaic redox processes in addition to EDL are known as pseudocapacitors or redox capacitors, exhibiting higher energy outputs by several orders of magnitude than EDLCs.[21] Metal oxides (RuO_2) and conducting polymers are two well-known pseudocapacitor materials.

1-3 Electroactive Organic Groups

Compared to their inorganic counterparts, organic compounds were not traditionally considered as an important class of electrode materials. In recent years, however, organics have made tremendous progress, drawing the attention of the EES community. Five major groups of molecules have evolved during the four decades of research efforts in the organic EES field. These groups presented below can be divided into 1) organic disulfides, 2) violenes, 3) nitroxides, 4) carbonyls, and 5) conducting polymers.

Organic Disulfides

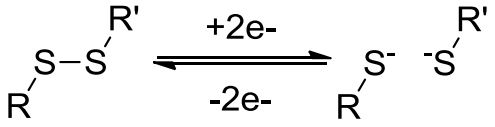

Figure 1-3. Redox property of organic disulfide.

Among the major classes of organic electrodes, organosulfur compounds with disulfide functionality offer the highest capacities (300 – 800mAh/g). This group was

first introduced into the field of EES by Visco et al. as alternative electrode materials in high temperature battery systems such as Na-Na_2S_X.[22] Organic disulfide compounds could be regarded as the organic version of sulfur-based electrodes. This type of material, bearing a disulfide functionality, goes through reversible redox reaction of reductive cleavage and oxidative disulfide formation (Figure 1-3). The most studied organic disulfide is 2,5-dimercapto-1,3,4-thiadiazole (DMcT) due to its high redox potential and theoretical capacity.[23] The physical and electrochemical properties can be manipulated depending on the R groups. For example, by changing the R group from electron-donating alkyl groups to electron-withdrawings aryl groups, the redox potentials can be shifted about 700mV (2.3 to 3.0V vs Li/Li^+).[24]

The main drawback of these materials is that they suffer from slow reductive cleavage of the disulfide bonds. Large separation between the cathodic and anodic peak potentials are observed in cyclic voltammetry, indicating sluggish redox kinetics. Electrocatalysts are required when operated at a lower temperature. It was reported that poly(3,4-ethylenedioxythiophene) (PEDOT) has a remarkable electrocatalytic activity towards the redox reaction of DMcT, in which the peak separation decreased significantly when a PEDOT-modified electrode was employed.[25-27] By including an electrocatalyst, organic disulfides with high capacity can potentially be one of the most promising organic EES materials.

Violenes

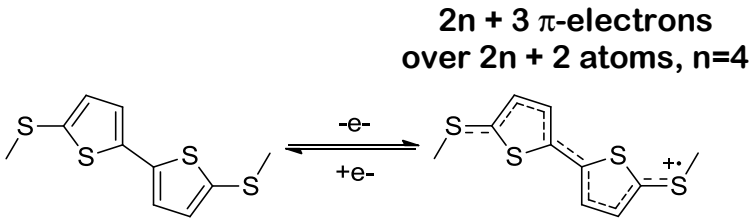

Figure 1-4. Redox property of violene, BMTbT.

Violene cations are conjugated molecules with the delocalization of 2n + 3 π-electrons over a 2n + 2 atom framework (Figure 1-4).[28] Many of these cations has been found to be stable over hours to even months.[29] The unusual stability of these cations can be explained from the high degree of charge delocalization. Two major advantages over the organic disulfides are 1) high redox potentials (>3.0V vs Li/Li^+) and 2) do not require electrocatalyst. Previously, our group has focused on a series of thioether-based redox-active molecules as potential cathode materials for supercapacitors.[30] 5,5'-Bis(methylthio)-2,2'-bithiophene, BMTbT (Figure 1-4) was determined to be a highly promising energy storage material as it is capable of providing two chemically and electrochemically reversible one-electron processes at very positive potentials (3.8 and 4.0 V vs. Li/Li^+) as well as a high theoretical gravimetric capacity (209 mAh/g). The theoretical energy density of BMTbT (836 Wh/kg) is considerably greater than traditional battery electrode materials such as $LiFePO_4$ (495 Wh/kg) and $LiCoO_2$ (518 Wh/kg).

Nitroxide (Organic Free Radical)

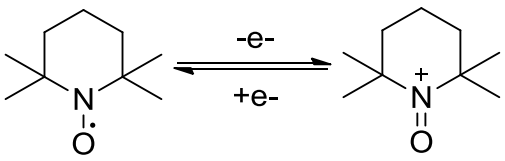

Figure 1-5. Redox property of nitroxide.

Nitroxide-based materials are the most studied radical compounds for electrode applications. Like the violenes, these are also cation-forming materials that can be oxidized at a high potential. A nitroxide such as 2,2,6,6-tetramethylpiperidine-1-oxyl (TEMPO) can be reversibly p-doped to the oxoammonium cation in an oxidation reaction (Figure 1-5). The first nitroxide-based cathode material, poly-(2,2,6,6-tetramethyl-peperidinyloxy-4-yl methacrylate) (PTMA) with a theoretical gravimetric capacity of 111

mAh/g, was reported by Nakahara et. al.[31] A flat discharge plateau at 3.5V vs Li/Li^+ was observed, which corresponded to the redox process of the pendant TEMPO units on the polymer. One notable feature of this radical cathode is the high-rate capability. However, these capacities tend to be on the lower side compared to the other redox-active organic groups.

Carbonyls

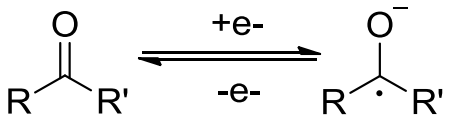

Figure 1-6. Redox property of carbonyl.

The carbonyl is a common organic functional group that shows reductive capability (Figure 1-6). Carbonyl compounds were among the earliest organic candidates for electrode materials in lithium-based batteries. In the 1960's, Williams et al. utilized dichloroisocyanuric acid as the cathode in a primary lithium battery.[32] Two discharge plateaus at 3.0 and 3.5V vs Li/Li^+ and a capacity of ~120 mAh/g were observed. Alt et al. were the first to attempt using chloranil as a rechargeable electrode material.[33] Other small carbonyl-based compounds such as anthraquinone were also attempted for secondary lithium batteries, but unsatisfactory results were obtained. High solubility in organic solvents translated to a rapid fade in the capacity. After these frustrating results, not many reports on carbonyl-based electrodes were reported till recently. Recent reports have focused on the polymerization[34-40] and the salt-formation[41-44] (enhancing polarity) of carbonyl compounds to mitigate the solubility issues. Many of these results did show significant improvement in charge-discharge cyclability. As these materials suffer from low reduction potentials (hence, voltage), increasing the potential is

a necessity for carbonyls to be competitive as electrode materials in the future.

Conducting Polymers

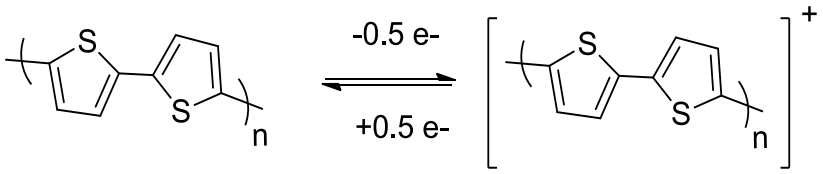

Figure 1-7. Redox property of conducting polymer.

Conducting polymers are attractive as electrode materials for electrochemical capacitors due to their ability to store charge in a pseudocapacitive manner and the insolubility in most organic solvents used as electrolytes. In fact, some devices based on conducting polymer materials (e.g. polythiophenes, Figure 1-7) have shown promise due to a fast doping/de-doping processes.[45-50] However, the capacities of these polymeric materials are low when compared to inorganic battery materials. The electrochemical reactions involve a fraction of an electron per monomer unit with the need for significant amounts of supporting electrolyte media, lowering the gravimetric capacity and energy density.[51-53] Nevertheless, conducting polymers are still receiving much attention as promising electrodes in electrochemical capacitors.

1-4 Addressing the Shortcomings of Organics – 'Hybrid' Approach

The previous section introduced four major discrete, non-polymeric electroactive organic groups. These compounds share several shortcomings, even though each individual possess different chemical motif. Foremost, high solubility in organic solvents translates to a rapid fade in the capacity of the EES device. Also, there arises a need to add a conducting additive as these molecules are generally insulators. Usually a large amount (50-80%) of conductive carbon is employed for the composite electrode. In the

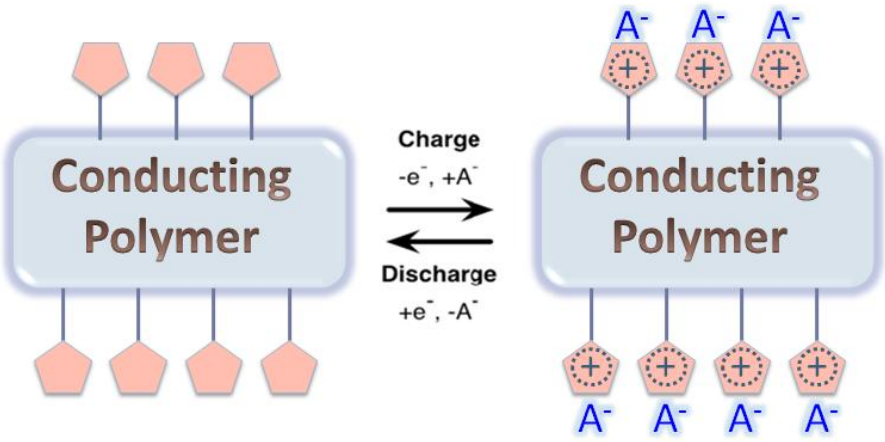

Figure 1-8. Schematic depiction of the 'hybrid' approach.

case of conducting polymers, these materials are conductive and insoluble, but suffer from very low capacities due to the fractional electron obtainable from each monomer unit. The major part of this dissertation is addressing these issues by utilizing a 'hybrid' approach (Figure 1-8) by binding these promising small organic molecules onto an insoluble conducting polymer through organic synthesis to avoid dissolution and obtain conductivity. An alternative view of this approach can be seen as an enhancement of the energy density of conducting polymers by increasing the charge to weight ratio with electroactive pendant additives. As the use of 'hybrid' materials is almost none existent in literature, the application of these novel materials could well play a crucial role in current and emerging EES technologies, competing and outperforming traditional electrode materials.

1-5 Dissertation Overviews

The emergent need to find successful electrical energy storage systems, maximize capacity and energy density per unit mass (or volume) and decrease cost, naturally led to examining organic materials as a potential solution. Organic molecules are composed of widely-available, lightweight elements, and their properties can be rationally tuned using

well-established principles of organic chemistry. Moreover, both amorphous and crystalline organic materials can accommodate more dramatic changes in volume than the inorganic systems currently being proposed for next-generation batteries. The primary focus of this dissertation is on the organic synthesis and electrochemical characterization of new redox-active organic materials for developing the next generation high-energy cathode materials for EES devices.

All experimental information and procedures are outlined in Chapter 2. It is divided into five sections: Reagents and Materials, Electrochemical Measurements, Device Testing, Computational Methods, and Synthesis.

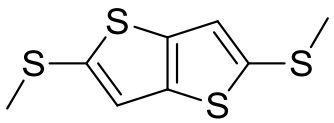

Figure 1-9. 2,5-Bis(methylthio)thieno[3,2-*b*]thiophene **(**FBMTbT).

Chapter 3 focuses on identification, synthesis, and characterization of new organosulfurs as potential pseudocapacitive electrode materials suitable for high power applications. Cyclic voltammetry (CV) and rotating disk electrode (RDE) voltammetry were used to evaluate the electrochemical properties of these compounds. These fundamental electrochemical evaluations are necessary for the advancement of novel materials for EES applications. 2,5-Bis(methylthio)thieno[3,2-*b*]thiophene **(**FBMTbT, Figure 1-9) was thoroughly studied as the most promising candidate due to its multiple reversible redox processes occurring at high positive potentials and its high rate capability.

Chapters 4 and 5 center on the synthesis, characterization, and device-level testing of hybrid-type materials based on *p*-phenylenediamine for supercapacitor applications.

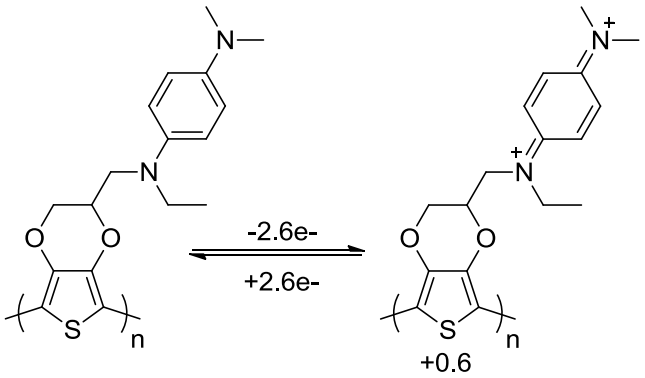

Figure 1-10. Redox property of poly-(EDOT-TAPD).

Poly-3,4-ethylenedioxythiophene (PEDOT)/*N*,*N*,*N*′,*N*′-tetraalkylated-*p*-phenylene-diamine (TAPD) composite (poly-(EDOT-TAPD), Figure 1-10), which can exchange up to 2.6 electrons per monomer unit, has been synthesized and thoroughly characterized displaying promising results as early studies indicate good electrochemical cyclability and performance. Electrosynthesis was utilized to deposit a porous poly-(EDOT-TAPD) film directly onto the current collector using a potential step method. The early device testing exhibited capacities approximately twice that of a pure PEDOT film. While further improvement of the cycling performance is necessary for practical applications, this preliminary work from these two chapters demonstrated a feasible methodology to prepare organic electrode materials with excellent energy densities for EES.

The 'hybrid' approach from Chapters 4 and 5 is applied to organic disulfide LIB materials in Chapter 6. This chapter outlines a methodology to attach 2,5-dimercapto-1,3,4-thiadiazole (DMcT) molecules directly to PEDOT backbone using a post-polymerization modification method (Figure 1-11). Similar to many other small organics, DMcT is also soluble in common battery electrolyte solutions, resulting in poor cyclability for composite electrodes. It is a necessity for these active species to remain in

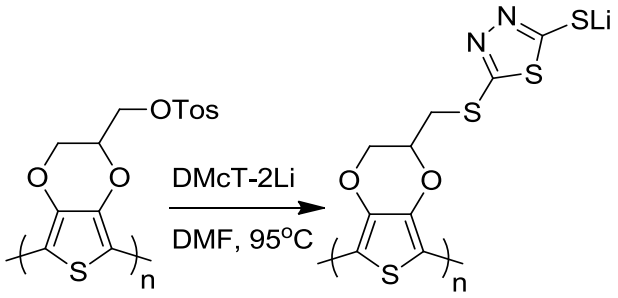

Figure 1-11. Post-polymerization reaction: DMcT confinement on PEDOT.

contact with the electrode. Early studies indicate high incorporation of DMcT onto PEDOT and excellent electrochemical cyclability.

Finally, Chapter 7 concludes the dissertation with summary and recommendation for future research directions with regards to organic electrodes.

1-6 References

1. H. Chen, M. Armand, G. Demailly, F. Dolhem, P. Poizot and J.-M. Tarascon, *ChemSusChem*, 2008, **1**, 348.
2. J.-M. Tarascon, *Phil. Trans. R. Soc. A*, 2010, **368**, 3227.
3. H. Chen, M. Armand, M. Courty, M. Jiang, C. P. Grey, F. Dolhem, J.-M. Tarascon and P. Poizot, *J. Am. Chem. Soc.*, 2009, **131**, 8984.
4. W. Walker, S. Grugeon, O. Mentre, S. Laruelle, J.-M. Tarascon and F. Wudl, *J. Am. Chem. Soc.*, 2010, **132**, 6517.
5. R. Gracia and D. Mecerreyes, *Polym. Chem.*, 2013, **4**, 2206.
6. T. Nakajima, *J. Fluorine Chem.*, 1999, **100**, 57.
7. H. Chen, T. N. Cong, W. Yang, C. Tan, Y. Li and Y. Ding, *Prog. Nat. Sci.*, 2009, **19**, 291.
8. H. D. Abruña, Y. Kiya and J. C. Henderson, *Phys. Today*, 2008, **61**, 43.

9. T. Christen and M. W. Carlen, *J. Power Sources*, 2000, **91**, 210.

10. D. Berndt, *J. Power Sources*, 2001, **100**, 29.

11. S. Tobishima, K. Takei, Y. Sakurai and J. Yamaki, *J. Power Sources*, 2000, **90**, 188.

12. J. Chen, L. Xu, W. Li and X. Gou, *Adv. Mater.*, 2005, **17**, 582.

13. C. K. Chan, H. Peng, G. Liu, K. McIlwrath, X. F. Zhang, R. A. Huggins and Y. Cui, *Nat. Mater.*, 2008, **3**, 31.

14. J. O. Besenhard, J. Yang and M. Winter, *J. Power Sources*, 1997, **68**, 87.

15. P. Poizot, S. Laruelle, S. Grugeon, L. Dupont and J.-M. Tarascon, *Nat. Mater.*, 2000, **407**, 496.

16. E. Frackowiak and F. Beguin, *Carbon*, 2001, **39**, 937.

17. C. Arbizzani, M. Mastragostino and F. Soavi, *J. Power Sources*, 2001, **100**, 164.

18. B. E. Conway, V. Birss and J. Wojtowicz, *J. Power Sources*, 1997, **66**, 1.

19. B. E. Conway, *Electrochemical Supercapacitors-Scientific Fundamentals and Technological Applications*, Kluwer Academic: New York, 1999.

20. D. Galizzioli, F. Tantardini and S. Trasatti, *J. Appl. Electrochem.*, 1974, **4**, 57.

21 P. Simon and Y. Gogotsi, *Nat. Mater.*, 2008, **7**, 845.

22. S. J. Visco, C. C. Mailhe, L. C. De Jonghe and M. B. Armand, *J. Electrochem. Soc.*, 1989, **136**, 661.

23. S. Picart and E. Genies, *J. Electroanal. Chem.*, 1996, **408**, 53.

24. M. Liu, S. J. Visco and L. C. De Jonghe, *J. Electrochem. Soc.*, 1991, **138**, 1896.

25. N. Oyama, Y. Kiya, O. Hatozaki, S. Morioka and H. D. Abruña, *Electrochem. Solid St.*, 2003, **6**, A286.

26. Y. Kiya, O. Hatozaki, N. Oyama and H. D. Abruña, *J. Phys. Chem. C*, 2007, **111**, 13129.

27. G. G. Rodriguez-Calero, M. A. Lowe, Y. Kiya and H. D. Abruña, *J. Phys. Chem. C*, 2010, **114**, 6169.

28. S. Hunig, *Pure Appl. Chem.*, 1967, **15**, 109.

29. L. Michaelis, M. P. Schubert and S. Granick, *J. Am. Chem. Soc.*, 1939, **61**, 1981.

30. J. C. Henderson, Y. Kiya, G. R. Hutchison and H. D. Abruña, *J. Phys. Chem. C*, 2008, **112**, 3989.

31. K. Nakahara, S. Iwasa, M. Satoh, Y. Morioka, J. Iriyama, M. Suguro and E. Hasegawa, *Chem. Phys. Lett.*, 2002, **359**, 351.

32. D. L. Williams, J. J. Byrne and J. S. Driscoll, *J. Electrochem. Soc.*, 1969, **116**, 2.

33. H. Alt, H. Binder, A. Kohling and G. Sandstede, *Electrochim. Acta*, 1972, **17**, 873.

34. Z. Song, H. Zhan and Y. Zhou, *Chem. Commun.*, 2009, 448.

35. Z. Song, H. Zhan and Y. Zhou, *Agnew. Chem.*, 2010, **122**, 8622.

36. J. Geng, J.-P. Bonnet, S. Renault, F. Dolhem and P. Poizot, *Energy Environ. Sci.*, 2010, **3**, 1929.

37. K. Liu, J. Zheng, G. Zhong and Y. Yang, *J. Mater. Chem.*, 2011, **21**, 4125.

38. D. Haringer, P. Novak, O. Haas, B. Piro and M.-C. Pham, *J. Electrochem. Soc.*, 1999, **146**, 2393.

39. Z.-Y. Tang and G.-X. Xu, *Acta Phys. Chim. Sin.*, 2003, **19**, 307.

40. G. Xu, L. Qi, L. Wen, G. Liu and Y. Ci, *Acta Polym. Sin.*, 2006, 795.

41. J. Xiang, C. Chang, M. Li, S. Wu, L. Yuan and J. Sun, *Cryst. Growth Des.*, 2008, **8**, 280.

42. S. Renault, J. Geng, F. Dolhem and P. Poizot, *Chem. Commun.*, 2011, **47**, 2414.

43. R.-H. Zeng, X.-P. Li, Y.-C. Qiu, W.-S. Li, J. Yi, D.-S. Lu, C.-L. Tan and M.-Q. Xu, *Electrochem. Commun.*, 2010, **12**, 1253.

44. H. Chen, P. Poizot, F. Dolhem, N. I. Basir, O. Mentre and J.-M. Tarascon, *Electrochem. Solid-State Lett.*, 2009, **12**, A102.

45. G. Wang, L. Zhang and J. Zhang, *Chem. Soc. Rev.*, 2012, **41**, 797.

46. M. Mastragostino, C. Arbizzani and F. Soavi, *J. Power Sources*, 2001, **97-98**, 812.

47. K. S. Ryu, Y. Lee, K.-S. Han and M. G. Kim, *Mater. Chem. Phys.*, 2004, **84**, 380.

48. K. Gurunathan, A. V. Murugan, R. Marimuthu, U. P. Mulik and D. P. Amalnerkar, *Mater. Chem. Phys.*, 1999, **61**, 173.

49. G. A. Snook, P. Kao and A. S. Best, *J. Power Sources*, 2011, **196**, 1.

50. A. Burke, *J. Power Sources*, 2000, **91**, 37.

51. M. Mastragostino, C. Arbizzani and F. Soavi, *Solid State Ionics*, 2002, **148**, 493.

52. P. Novak, K. Muller, K. S. V. Santhanam and O. Haas, *Chem. Rev.*, 1997, **97**, 207.

53. G. Zotti, S. Zecchin and G. Schiavon, *Chem. Mater.*, 2000, **12**, 2996.

CHAPTER TWO

EXPERIMENTAL

2-1 Reagents and Materials

Acetic acid, anthraquinone, azobisisobutyronitrile (AIBN), benzene, bromoethane, 3-bromo-1,2-propanediol, *N*-bromosuccinimide (NBS), *n*-butyllithium (1.6M and 2.5M in hexanes), copper(II) chloride dihydrate, copper(II) oxide, 3,4-dibromothiophene, *N*,*N*-dicyclohexylcarbodiimide, 2,5-dimercapto-1,3,4-thiadiazole, 2,5-dimethoxytetrahydrofuran, 3,4-dimethoxythiophene, 4-(dimethylamino)pyridine, dimethyldisulfide, *N*,*N*-dimethyl-p-phenylenediamine, *N*,*N'*-diphenylethylenediamine, 1,2-ethanedithiol, ethanol, 3,4-ethylenedioxythiophene, isopropanol, lithium bis(trifluoromethane)sulfonimidate (LiTFSI), lithium hydroxide, lithium perchlorate ($LiClO_4$), magnesium sulfate, 4-nitrobenzenediazonium tetrafluoroborate, 9-phenylanthracene, potassium carbonate, potassium iodide, propylene carbonate (PC), sodium hypophosphite monohydrate, tetrabutylammonium hexafluorophosphate (TBAH), tetrabutylammonium perchlorate (TBAP), tetraglyme, tetrakis-(triphenylphosphine) palladium, thieno[3,4-b]-1,4-dioxin-2-methanol, 2-thienyllithium (1.0M in THF and hexanes), tin(II) chloride, *p*-toluenesulfonic acid monohydrate, *p*-toluenesulfonyl chloride, triethylamine, and 4-vinylphenylboronic acid were purchased from Sigma-Aldrich. Acetonitrile (AN), chloroform, dichloromethane, diethyl ether (ether), *N*,*N*-dimethylformamide (DMF), hexane, sodium carbonate, sodium hydroxide, sodium sulfate, tetrahydrofuran (THF), and toluene were acquired from Fisher Scientific. Acetone, methanol, and sodium chloride were obtained from Macron Chemicals. 1-(2-

Bromoethyl)pyrrole and thieno[3,2-b]thiophene were purchased from TCI America. Prepurified argon and nitrogen gases were acquired from Airgas. Silica Gel 60, Tokai 5500 Carbon Black, and alumina were obtained from EMD Chemicals, Tokai Carbon, and Refine Tec, respectively. All of the chemicals mentioned above were used as received.

2-2 Electrochemical Measurements

All electrochemical measurements were performed by Dr. Stephen Burkhardt (Compound **4**) and Gabriel Rodriguez-Calero. Cyclic voltammetry (CV) studies were carried out at room temperature using a Hokuto Denko Co., HABF1510m potentiostat. Rotating-disk electrode (RDE) voltammetric studies were carried out at room temperature using a Pine Instruments Co. model AFMSRX rotator and a Hokuto Denko Co., HABF1510m potentiostat. In RDE studies, linear sweeps were performed at 10 mV/s at different rotation rates. Measurements were taken in a three-electrode cell configuration using a 3mm diameter homemade glassy carbon disk electrode (GCE), a large area Pt coil counter electrode, and a Ag/Ag^+ (0.05 M $AgClO_4$ + 0.1 M $LiClO_4$/AN) reference electrode without regards to the liquid junction potential, and against, unless otherwise noted, all potentials are reported. The working electrode was polished with 1.0 μm, 0.3 μm, and 0.05 μm alumina slurries, rinsed with distilled water and acetone (or isopropanol), and dried prior to use. It was then electrochemically cleaned by cycling the potential in a 1 M NaOH solution between 0.0 V and +1.3 V versus Ag/AgCl (KCl saturated), followed by rinsing with distilled water and acetone (or isopropanol). All solutions were thoroughly purged for at least 10 minutes with prepurified nitrogen gas prior to use.

2-3 Device Testing

The device testing was performed by Dr. Jie Gao. CR2032 coin cells were used to evaluate the charge/discharge performance of the poly-(EDOT-TAPD) hybrid electrode. The directly polymerized electrode was cut into a disc with a diameter of 1.1 cm and used as the cathode. Coin cells were assembled in an argon-filled glove box with lithium foil as the anode, Celgard 2320 as the separator, 1.0 M LiTFSI in TEGDME as the electrolyte. The cells were galvanostatically charged and discharged with a current density of 50 mA/g between 3 to 4.2V using an Arbin model battery charger.

2-4 Computational Methods

All computational studies were performed by Dr. Stephen Burkhardt. Initially, all small molecules were relaxed using the Universal Force Field (UFF) as implemented in the Avogadro 1.0 software program.[1] Resulting geometries were then relaxed without constraints using Gaussian09, revision A.02 at the level of density functional theory (DFT). [2, 3] Structure optimizations were performed using the B3LYP hybrid functional,[4] with the 6-31+G(d,p) basis set and the conductor polarizable continuum model (PCM) for acetonitrile solution.[5, 6] The B3LYP hybrid functional was used based on good agreement for enthalpies of formation[7], ionization potentials and electron affinities[8], and band gaps[9] with experimental data. Images of molecules and isosurfaces were produced with GaussView 5.0.

2-5 Synthesis

^{1}H NMR and ^{13}C NMR were acquired on a Bruker ARX300 or a Varian Mercury-300 spectrometer using $CDCl_3$ or DMSO-d_6. IR spectra were obtained on a *Thermo Electron's Nicolet Avatar 370 DTGS or Thermo Scientific's* Nicolet iS10 FT-IR

spectrometer. Spectra were recorded in ∂ (ppm) for NMR and wavenumbers (cm^{-1}) for IR.

Chapter Three

5,7-Bis(methylthio)-2,3-dihydrothieno[3,4-b][1,4]dioxine (*2*). To a solution of 2,3-dihydrothieno[3,4-b][1,4]dioxine (0.5g, 3.52mmol) in THF (5.5mL) under nitrogen was added *n*-butyllithium (4.4mL, 7.04mmol, 1.6M in hexanes) at -78^{o}C dropwise via syringe. The reaction mixture was allowed to stir at -78 ^{o}C for 1hr, after which dimethyldisulfide (0.62mL, 7.04mmol) dissolved in THF (15mL) was added dropwise. The solution was warmed slowly to room temperature and allowed to stir for 4hrs. Then, the reaction mixture was diluted with hexanes, and the organic layer was washed with water and brine. The organic layer was dried with Na_2SO_4, and concentrated under reduced pressure to afford a crude oil that was further purified by column chromatography over silica gel using hexanes to 9:1 hexanes/ethyl acetate mixture to afford **2** as a white crystalline solid (0.2 g, 24.2%). ^{1}H NMR (300 MHz, $CDCl_3$): ∂ 4.26 (s, 4H), 2.37 (s, 6H).

3,4-Dimethoxythiophene.[10] Sodium (16.1g, 0.70mol) was added in small portions to absolute methanol (225mL) under an argon atmosphere. After stirring for 30min, KI (0.250g, 1.5mmol), 3,4-dibromothiophene (33.9g, 0.14mol), and CuO (11.2g, 0.14mol) were added. The reaction mixture was refluxed for 4 days. Once cooled to room temperature, the solution was filtered, diluted with water, and extracted with ether. The combined organic layers were dried with Na_2SO_4 and concentrated under reduced pressure to afford an oil. The crude oil was purified by vacuum distillation to afford a slightly yellow liquid (13.2 g, 65.4%). ^{1}H NMR (300 MHz, $CDCl_3$): ∂ 6.19 (s, 2H), 3.86

(s, 6H).

2,3-dihydrothieno[3,4-b][1,4]dithiine.[11] 3,4-Dimethoxythiophene (3.00g, 20.8mmol), 1,2-ethanedithiol (19.6g, 208mmol), *p*-toluenesulfonic acid monohydrate (0.34g, 1.79mmol), and toluene (60mL) were mixed under nitrogen. The reaction mixture was heated at 90^{o}C for 3.5 days. Once cooled to room temperature, toluene was removed, and the oil was diluted with ether. The organic layer was washed with 6.5% $NaOH_{(aq)}$ and then water. The solution was dried with Na_2SO_4 and concentrated under reduced pressure to afford an oil. The crude oil was purified by vacuum distillation and then through column chromatography over silica gel using 5:1 to 3:1 hexanes/dichloromethane mixture to give a clear oil (1.57g, 43.3%). ^{1}H-NMR (300 MHz, $CDCl_3$): ∂ 6.96 (s, 2H), 3.21 (s, 4H).

5,7-bis(methylthio)-2,3-dihydrothieno[3,4-b][1,4]dithiine (*3*). To a solution of 2,3-dihydrothieno[3,4-b][1,4]dithiine (0.595g, 3.42mmol) in THF (12mL) under nitrogen was added *n*-butyllithium (4.3mL, 6.85mmol, 1.6M in hexanes) at -78^{o}C dropwise via syringe. The reaction mixture was allowed to stir at -78^{o}C for 1hr, after which dimethyldisulfide (0.60mL, 6.85mmol) was added dropwise. The solution was stirred for an additional 3hrs, warmed slowly to room temperature, and then allowed to stir for 12hrs. The reaction mixture was diluted with ether and washed with water. The organic layer was dried with Na_2SO_4 and concentrated under reduced pressure to afford a crude oil that was further purified by column chromatography over silica gel using 5:1 hexanes/chloroform as to afford **3** as a brownish-oil (0.393g, 43.1%). ^{1}H NMR (300 MHz, $CDCl_3$): ∂ 3.22 (s, 4H), 2.39 (s, 6H).

2,5-Bis(methylthio)thieno[3,2-*b*]thiophene (*4*).[12] To a solution of thieno[3,2-b]-

thiophene (0.5g, 3.57mmol) in THF (12mL) under nitrogen was added *n*-butyllithium (3.3mL, 8.2mmol, 2.5M in hexanes) at -78^{o}C dropwise via syringe. The reaction mixture was allowed to stir at -78^{o}C for 1.5hrs, after which dimethyldisulfide (1.46mL, 16.4mmol) was added dropwise via syringe. The solution was stirred for an additional 1.5hrs, and warmed slowly to room temperature, and allowed to stir for 6hrs. Then, the reaction mixture was diluted with water, and the aqueous layer was extracted with ether. The combined organic layers were dried with Na_2SO_4 and concentrated under reduced pressure to afford a crude solid that was further purified by column chromatography over silica gel using hexanes as elutent to afford **4** as a white crystalline solid (0.3g, 36.2%). ^{1}H NMR (300 MHz, $CDCl_3$): ∂ 7.19 (s, 2H), 2.52 (s, 6H).

Chapter Four

***N*-Ethyl-*N*',*N*'-dimethyl-*p*-phenylenediamine.**[13] Following a modified literature procedure, *n*-butyllithium (6.30mL, 15.7mmol, 2.50M in hexanes) was added dropwise at -78^{o}C to a solution of *N*,*N*-dimethyl-*p*-phenylenediamine (2.00g, 14.7mmol) dissolved in THF (100mL) under argon. The reaction mixture was allowed to stir at -78^{o}C for 45min, after which bromoethane (1.10mL, 14.9mmol) was added dropwise. The solution was stirred for an additional 20min., warmed slowly to room temperature, and allowed to stir overnight. The reaction mixture was diluted with ether and washed with water and brine. The organic layer was dried with Na_2SO_4 and concentrated under reduced pressure to afford a dark colored oil that was further purified by column chromatography over silica gel using 4:1 to 3:2 hexanes/ethyl acetate mixture to give the product as a red oil (1.27g, 52.7%). IR (Neat): 3380.5, 3051.0, 3016.3, 2968.2, 2871.3, 1618.4, 1518.0 cm^{-1}. ^{1}H-NMR (300 MHz, DMSO-d_6): ∂ 6.61 (d, 2H), 6.47 (d, 2H), 4.77 (s, 1H), 2.93 (q, 2H),

2.68 (s, 6H), 1.11 (t, 3H). ^{13}C-NMR (300 MHz, DMSO-d_6): ∂ 143.2, 142.0, 115.8, 113.7, 42.3, 38.7, 15.1.

2-(Bromomethyl)-2,3-dihydrothieno[3,4-b][1,4]dioxine. 3,4-Dimethoxythiophene (5.13g, 35.6mmol), 3-bromo-1,2-propanediol (4.85g, 31.3mmol), *p*-toluenesulfonic acid monohydrate (1.50g, 7.89mmol), and toluene (80mL) were mixed under argon. The reaction mixture was heated at 100^{o}C for 21hrs and then allowed to cool to room temperature. A black insoluble material was filtered out, and the solution was diluted with dichloromethane. The organic layer was washed with water and brine. The solution was then dried with $MgSO_4$ and concentrated under reduced pressure to afford a black oil. The crude oil was purified by column chromatography over silica gel using 3:1 hexanes/dichloromethane to give a clear oil, which upon cooling solidified into a white solid (2.97g, 40.4%). IR (Neat): 3112.9, 3035.7, 2996.2, 2929.3, 1579.6 cm^{-1}. ^{1}H-NMR (300 MHz, $CDCl_3$): ∂ 6.37 (s, 2H), 4.39 (dtd, 1H), 4.30 (dd, 1H), 4.17 (dd, 1H), 3.52 (m, 2H). ^{13}C-NMR (300 MHz, $CDCl_3$): ∂ 141.1, 140.7, 100.1, 72.6, 66.2, 28.6.

1-(4-dimethylamino)pyrrole (*6*).[14] Following a literature procedure for a similar product, a solution of 2,5-dimethoxytetrahydrofuran (1.29mL. 9.96mmol) and *N*,*N*-dimethyl-*p*-phenylenediamine (1.32g, 9.69mmol) dissolved in 20mL of acetic acid was refluxed for 30min. Subsequently, 10mL of acetic acid were added. After 5min., carbon black was added and the mixture was refluxed for another 10min. The carbon was filtered off and the acetic acid was removed under reduced pressure. The residue was dissolved in ether and washed with 1M $NaOH_{(aq)}$. The organic layer was concentrated in vacuum and purified by column chromatography over silica gel using 1:3:1 to 2:7:1 chloroform/ hexane/ethyl acetate mixture. This was then further purified by

recrystallizing from ethanol to afford a white solid (0.280g, 15.5%). IR (Neat): 3134.3, 3100.9, 3053.6, 2981.3, 2851.0, 1611.8 cm^{-1}. ^{1}H-NMR (300 MHz, $CDCl_3$): ∂ 7.25 (m, 2H), 6.98 (t, 2H), 6.75 (m, 2H), 6.30 (t, 2H), 2.96 (s, 6H). ^{13}C-NMR (300 MHz, $CDCl_3$): ∂ 149.0, 131.2, 119.8, 113.1, 109.3, 40.8.

General Preparation of Compounds 7-9. Phenylenediamine, functionalizable monomer, and $NaHCO_3$ were mixed in DMF under argon. The reaction mixture was stirred at 90°C for 20hrs. The solution was diluted with ethyl acetate after cooling to room temperature and then washed with water and brine. The solvent was removed under vacuum. The crude material was purified by column chromatography over silica gel using 3:2 hexanes/ethyl acetate to afford an oil.

***N*-(2-(1*H*-pyrrol-1-yl)ethyl)-*N*-ethyl-*N'*,*N'*-dimethyl-*p*-phenylenediamine (*7*).** *N*-Ethyl-*N*',*N*'-dimethyl-*p*-phenylenediamine (0.660g, 4.02mmol), 1-(2-bromoethyl)pyrrole (0.700g, 4.02mmol), $NaHCO_3$ (0.680g, 8.04mmol), and 20mL of DMF were used. Clear orange oil (0.343g, 33.1%). IR (Neat): 3097.8, 3047.2, 2969.7, 2872.0, 1611.9, 1518.5 cm^{-1}. ^{1}H-NMR (300 MHz, DMSO-d_6): ∂ 6.70 (m, 6H), 5.97 (t, 2H), 3.94 (t, 2H), 3.41 (s, 2H), 3.08 (s, 2H), 2.73 (s, 6H), 0.92 (t, 3H). ^{13}C-NMR (300 MHz, DMSO-d_6): ∂ 143.5, 140.2, 121.2, 115.6, 115.1, 108.1, 52.8, 47.2, 45.6, 41.9, 12.5.

***N*-((2,3-dihydrothieno[3,4-b][1,4]dioxin-2-yl)methyl)-*N'*,*N'*-dimethyl-*p*-phenylenediamine (*8*).** *N*,*N*-Dimethyl-*p*-phenylenediamine (0.694g, 5.10mmol), 2-(bromomethyl)-2,3-dihydrothieno[3,4-b][1,4]dioxine (1.20g, 5.10mmol), $NaHCO_3$ (0.858g, 10.2mmol), and 45mL of DMF were used. Red oil (0.531g, 35.9%). IR (Neat): 3384.7, 3108.3, 3020.9, 2941.1, 2873.2, 1610.4, 1579.9 cm^{-1}. ^{1}H-NMR (300 MHz, DMSO-d_6): ∂ 6.58 (m, 6H), 5.15 (t, 1H), 4.28 (m, 2H), 3.98 (m, 1H), 3.22 (t, 2H), 2.69 (s,

6H). ^{13}C-NMR (300 MHz, DMSO-d_6): ∂ 143.9, 141.9, 140.9, 115.7, 113.9, 100.1, 77.8, 66.6, 44.5, 42.1.

***N*-((2,3-dihydrothieno[3,4-b][1,4]dioxin-2-yl)methyl)-*N*-ethyl-*N*',*N*'-dimethyl-*p*-phenylenediamine (*9*).** *N*-Ethyl-*N*',*N*'-dimethyl-*p*-phenylenediamine (0.699g, 4.25mmol), 2-(bromomethyl)-2,3-dihydrothieno[3,4-b][1,4]dioxine (1.00g, 4.25mmol), $NaHCO_3$ (0.715g, 8.51mmol), and 20mL of DMF were used. Clear yellow oil (0.332g, 24.6%). IR (Neat): 3108.4, 3047.9, 2969.3, 2870.2, 1612.1, 1580.1 cm^{-1}. ^{1}H-NMR (300 MHz, DMSO-d_6): ∂ 6.70 (d, 4H), 6.56 (s, 2H), 4.22 (m, 2H), 3.99 (dd, 1H), 3.36 (d, 2H), 3.26 (m, 2H), 2.73 (s, 6H), 0.98 (t, 3H). ^{13}C-NMR (300 MHz, DMSO-d_6): ∂ 144.0, 141.7, 140.2, 116.1, 115.3, 100.2, 72.4, 66.6, 51.3, 46.6, 41.8, 12.2.

Chapter Five

Electropolymerization of *N*-((2,3-dihydrothieno[3,4-b][1,4]dioxin-2-yl)methyl)-*N*-ethyl-*N*',*N*'-dimethyl-*p*-phenylenediamine (*9*) on glassy carbon electrode. Consecutive cycling between -0.5 to 1.1V vs Ag/Ag^+ was carried out on glassy carbon electrode in a solution containing 20mM of **9**, 0.1M TBAP in AN. The peak current, as well as the double layer capacitance increased, evidencing formation of a CP film on the electrode surface.

Electropolymerization of *N*-((2,3-dihydrothieno[3,4-b][1,4]dioxin-2-yl)methyl)-*N*-ethyl-*N*',*N*'-dimethyl-*p*-phenylenediamine (*9*) on Au coated Al current collector. Monomer **9** was electropolymerized on a Au coated Al current collector using double step chronoamperometry. The first potential was held at -0.5V vs Ag/Ag^+ for 30s, then a step to 1.2V vs Ag/Ag^+ was applied for 20min, followed by a step to -0.6V vs Ag/Ag^+. The solution was stirred with a magnetic stirrer during the course of the experiment.

5,5'-Dithiobis(1,3,4-thiadiazole-2-thiol).[15] 2,5-Dimercapto-1,3,4-thiadiazole (2.00g, 13.3mmol) was dissolved in 1:1 ethanol/water mixture (v/v, 170mL). The reaction mixture was left standing for 4 days and then filtered. The product was washed with water and hexane to obtain a bright yellow solid (1.83g, 91.5%). The Raman spectrum of the product matched exactly the one from the literature.[16]

1,2-bis(5-(((2,3-dihydrothieno[3,4-b][1,4]dioxin-2-yl)methyl)thio)-1,3,4-thiadiazol-2-yl)disulfane (*10*). 2-(Bromomethyl)-2,3-dihydrothieno[3,4-b][1,4]dioxine (0.200g, 0.85mmol), 5,5'-dithiobis(1,3,4-thiadiazole-2-thiol) (0.085g, 0.28mmol), and Na_2CO_3 (0.075g, 0.71mmol) were mixed in DMF (5mL) under argon. The reaction mixture was stirred at 100^{o}C for 24hrs. The solution was diluted with ethyl acetate after cooling to room temperature and then washed with water and brine. The solvent was removed under vacuum. The crude material was purified by column chromatography over silica gel using 4:1 hexanes/ethyl acetate to afford a solid product (0.041g, 24.2%). ^{1}H-NMR (300 MHz, DMSO-d_6): ∂ 6.59 (s, 2H), 4.49 (tdd, 1H), 4.30 (dt, 1H), 4.02 (ddd, 1H), 3.58 (m, 2H).

(2,3-Dihydrothieno[3,4-b][1,4]dioxin-2-yl)methyl-4-methylbenzenesulfonate (*11*). Thieno[3,4-b]-1,4-dioxin-2-methanol (0.50g, 2.90mmol), triethylamine (0.44g, 4.36mmol), 4-(dimethylamino)pyridine (7.0mg, 0.058mmol), and *p*-toluenesulfonyl chloride (0.66g, 3.48mmol) were mixed in dichloromethane (10mL) at 0^{o}C under argon. The reaction mixture was slowly warmed to room temperature and stirred for 31hrs. The solution was diluted with ether and washed with diluted $HCl_{(aq)}$, $NaHCO_{3(aq)}$, water, and brine. The organic layer was then dried with $MgSO_4$ and concentrated under reduced

pressure to afford a yellow oil. The crude oil was purified by column chromatography over silica gel using 1:2 hexanes/dichloromethane to give a white solid (0.71g, 74.9%). ^{1}H NMR (300 MHz, $CDCl_3$): ∂ 7.80 (d, 2H), 7.36 (d, 2H), 6.32 (d, 1H), 6.25 (d, 1H), 4.36 (m, 1H), 4.19 (m, 3H), 4.02 (m, 1H), 2.46 (s, 3H).

Dilithium 2,5-dimercapto-1,3,4-thiadiazole salt (*12*). 2,5-Dimercapto-1,3,4-thiadiazole (2.00g, 13.3mmol) and LiOH (0.701g, 29.3mmol) were dissolved in methanol (170mL) under argon. The reaction mixture was stirred for 17hrs and then concentrated under reduced pressure. The crude product was washed with water and dried under vacuum to afford a white solid (1.83g, 84.7%). The Raman spectrum of the product matched exactly the one from the literature.[16]

Poly-[Lithium 5-(((2,3-dihydrothieno[3,4-b][1,4]dioxin-2-yl)methyl)thio)-1,3,4-thiadiazole-2-thiolate] (*13*). The electrochemically-generated poly-**11** film on glassy carbon electrode was exposed to a 0.5M solution of **12** in DMF at 95ºC under an argon atmosphere. The reaction progress was monitored through cyclic voltammetry with the modified electrode placed in a **12** free solution at specific time intervals until no further incorporation of **12** was observed. The electrode was then washed with acetone and acetonitrile.

Chapter Seven

9-Bromo-10-phenylanthracene.[17] To a solution of 9-phenylanthracene (3.28g, 12.9mmol) dissolved in chloroform (200mL) was added *N*-bromosuccinimide (2.66g, 14.9mmol) in portions. The reaction mixture was warmed to 45^{o}C and stirred for 3.5hrs, after which the solution was concentrated under reduced pressure. The crude material was purified by column chromatography over silica gel using hexanes to afford the

product as a yellow solid (2.48 g, 57.7%). ^{1}H NMR (300 MHz, $CDCl_3$): ∂ 8.63 (d, 2H), 7.62 (m, 7H), 7.41 (m, 4H).

9-Phenyl-10-(4-vinylphenyl)anthracene.[18] A solution of 9-bromo-10-phenylanthracene (1.32g, 3.96mmol), 4-vinylphenylboronic acid (0.750g, 5.07mmol), tetrakis(triphenyl-phosphine) palladium (0.200g, 0.173mmol), and K_2CO_3 (1.80g, 13.0mmol) in a 5:2:1 solvent mixture of benzene, water, and ethanol (58mL) was refluxed under argon for 32hrs. The reaction mixture was filtered, washed with brine, and dried with Na_2SO_4. After the removal of the solvent, the crude material was purified by column chromatography over silica gel using hexanes to give a solid product (0.722g, 51.2%). ^{1}H NMR (300 MHz, $CDCl_3$): ∂ 7.74-7.30 (m, 17H), 6.90 (dd, 1H), 5.95 (d, 1H), 5.40 (d, 1H).

Poly-(vinyl-9,10-diphenylanthracene).[18] A solution of 9-phenyl-10-(4-vinylphenyl)-anthracene (0.200g, 3.96mmol) and AIBN (0.005g, 0.030mmol) dissolved in THF (10mL) was heated to 65^{o}C and stirred under argon for 17hrs. A precipitate was formed when the reaction mixture was poured into methanol. The crude product was washed with methanol and hexane to give a yellow solid (0.107g, 53.5%). ^{1}H NMR (300 MHz, $CDCl_3$): ∂ 7.80-6.60 (br, 17H), 2.82 (br, 1H), 2.21 (br, 2H).

9-(4-Nitrophenyl)-10-phenylanthracene.[19] A solution of 4-nitrobenzenediazonium tetrafluoroborate in water (100mL) was poured into another solution of 9-phenylanthracene (2.54g, 10.0mmol) and copper(II) chloride dihydrate (7.11g, 30.0mmol) in acetone. The reaction mixture was heated to 35^{o}C and stirred for 2hrs. The solution was stored in the fridge overnight. The filtered solid was recrystallized using 1:1 ethanol/benzene to afford the product as a yellow crystalline solid (1.82g,

48.5%). The melting point (289.1-292.6 ^{o}C) matches the one from literature.

4-(10-Phenylanthracen-9-yl)aniline.[20] Tin(II) chloride (1.80g, mmol) in HCl (6.5mL) was added to a heated solution (95^{o}C) of 9-(4-nitrophenyl)-10-phenylanthracene (0.71g, 1.89mmol) in acetic acid (15mL). The reaction mixture was stirred for 1.5hrs. The filtered solid was washed with HCl and then suspended in 5% $NaOH_{(aq)}$ for 20min. The suspension was filtered to give a light yellow solid as a product (0.42g, 64.3%). ^{1}H NMR (300 MHz, DMSO-d_6): ∂ 7.73-7.36(m, 13H), 7.06 (d, 2H), 6.80 (d, 2H), 5.33 (s, 2H).

9,10-bis(2-thienyl)anthracene.[21] To a solution of anthraquinone (2.08g, 10.0mmol) in ether (150mL) under argon was added 2-thienyllithium (35mL, 35.0mmol, 1.0M in THF/hexanes) at -78^{o}C dropwise via syringe. The solution was warmed slowly to room temperature and stirred for 24hrs. The reaction mixture was quenched with water. The organic layer was washed with water, dried with Na_2SO_4, and then concentrated under reduced pressure to afford a crude solid that was further purified by column chromatography over silica gel using dichloromethane as elutent. The obtained solid was redissolved in methanol and stored overnight in a fridge to afford 9,10-dihydroanthracene-9,10-dithienyl-9,10-diol as a beige crystalline solid (0.507g, 13.5%). 9,10-Dihydroanthracene-9,10-dithienyl-9,10-diol (0.457g, 1.22mmol), KI (1.83g, 11.0mmol), and sodium hypophosphite monohydrate (2.20g, 20.8mmol) were dissolved in acetic acid (15mL) and refluxed for 2.5 hrs. Once cooled to room temperature, water was added to the reaction mixture. The precipitate was washed with water and methanol to give a yellow solid product (0.367g, 87.8%). ^{1}H NMR (300 MHz, $CDCl_3$): ∂ 7.88 (dd, 4H), 7.64 (d, 2H), 7.43 (dd, 4H), 7.33 (t, 2H), 7.24 (d, 2H).

N-Acetyl-N',N'-dimethylbenzene-1,4-diamine. To a solution of *N*,*N*-dimethyl-*p*-

phenylenediamine (1.00g, 7.4mmol) and triethylamine (2.05mL, 14.7mmol) in ether (22mL) under nitrogen was added acetyl chloride (1.04mL, 14.7mmol) at 0°C dropwise via syringe. The reaction mixture was allowed to stir at 0°C for 25min. The solution was warmed slowly to room temperature and allowed to stir for 9hrs. Then, the reaction mixture was quenched with water and extracted with ethyl acetate. The organic layer was washed with saturated $NaHCO_3$, water, and then brine. The solution was dried with $MgSO_4$ and concentrated under reduced pressure to afford a crude solid that was purified by column chromatography over silica gel using ethyl acetate as elutent and recrystrallizing twice with water to afford the product as a light yellow solid (0.201g, 15.6%). ^{1}H NMR (300 MHz, DMSO-d_6): ∂ 9.59 (s, 1H), 7.35 (d, 2H), 6.64 (d, 2H), 2.80 (s, 6H), 1.95 (s, 3H).

Covalent attachment of *N*,*N*-dimethyl-*p*-phenylenediamine composite on carbon black.[22] Tokai 5500 Carbon Black (0.10g, 8.33mmol), *N*,*N*-dimethyl-*p*-phenylenediamine (0.14g, 1.0mmol), N,N-dicyclohexylcarbodiimide (0.14g, 0.68mmol), and THF (10mL) were mixed under nitrogen. The reaction mixture was warmed to 35°C and stirred for 34hrs. Once cooled to room temperature, a black insoluble material was filtered out and washed with THF, acetone, and ether to obtain the final composite product (0.72g).

N,N'-Diethyl-N,N'-diphenylethane-1,2-diamine. N,N'-Diphenylethylenediamine (3.00g, 14.1mmol), bromoethane (6.16g, 56.5mmol), and $NaHCO_3$ (4.75g, 56.5mmol) were mixed in DMF (25mL) under argon. The reaction mixture was stirred at 85°C for 23hrs. Additional bromoethane (3.08g, 28.2mmol) was added to the reaction mixture, which was stirred for another 24hrs. The solution was diluted with ethyl acetate after

cooling to room temperature and then washed with water and brine. The solvent was removed under vacuum. The crude material was purified by column chromatography over silica gel using 7:3 hexanes/dichloromethane to afford a yellow solid. This was further purified by recrystallizing with methanol to give a white crystalline solid as a product (1.97g, 51.9%). ^{1}H NMR (300 MHz, $CDCl_3$): ∂ 7.26 (m, 4H), 6.72 (m, 6H), 3.51 (s, 4H), 3.41 (q, 4H), 1.17 (t, 6H).

2-6 References

1. *Avogadro: An Advanced Molecular Editor Designed for Cross-Platform use in Computational Chemistry, Molecular Modeling, Bioinformatics, Materials Science, and Related Areas*, http://avogadro.openmolecules.net/wiki/

2. M. J. Frisch, G. W. Trucks, H. B. Schlegel, G. E. Scuseria, M. A. Robb, J. R. Cheeseman, J. A. Montgomery, Jr., T. Vreven, K. N. Kudin, J. C. Burant, J. M. Millam, S. S. Iyengar, J. Tomasi, V. Barone, B. Mennucci, M. Cossi, G. Scalmani, N. Rega, G. A. Petersson, H. Nakatsuji, M. Hada, M. Ehara, K. Toyota, R. Fukuda, J. Hasegawa, M. Ishida, T. Nakajima, Y. Honda, O. Kitao, H. Nakai, M. Klene, X. Li, J. E. Knox, H. P. Hratchian, J. B. Cross, V. Bakken, C. Adamo, J. Jaramillo, R. Gomperts, R. E. Stratmann, O. Yazyev, A. J. Austin, R. Cammi, C. Pomelli, J. Ochterski, P. Y. Ayala, K. Morokuma, G. A. Voth, P. Salvador, J. J. Dannenberg, V. G. Zakrzewski, S. Dapprich, A. D. Daniels, M. C. Strain, O. Farkas, D. K. Malick, A. D. Rabuck, K. Raghavachari, J. B. Foresman, J. V. Ortiz, Q. Cui, A. G. Baboul, S. Clifford, J. Cioslowski, B. B. Stefanov, G. Liu, A. Liashenko, P. Piskorz, I. Komaromi, R. L. Martin, D. J. Fox, T. Keith, M. A. Al-Laham, C. Y. Peng, A. Nanayakkara, M. Challacombe, P. M. W. Gill, B. G.

Johnson, W. Chen, M. W. Wong, C. Gonzalez and J. A. Pople, *GAUSSIAN 03 (Revision C.02)*, Gaussian, Inc., Wallingford, CT, 2004

3. W. Kohn and L. Sham, *Phys. Rev. A*, 1964, **140**, 1133.
4. (*a*) A. D. J. Becke, *Chem. Phys.*, 1993, **98**, 5648. (*b*) C. Lee, W. Yang and R. G. Parr, *Phys. Rev. B*, 1988, **37**, 785.
5. M. Cossi, N. Rega, G. Scalmani and V. Barone, *J. Comput. Chem.*, 2003, **24**, 669.
6. V. Barone and M. Cossi, *J. Phys. Chem. A*, 1998, **102**, 1995.
7. L. A. Curtiss, K. Raghavachari, P. C. Redfern and J. A. Pople, *Chem. Phys. Lett.*, 1997, **270**, 419.
8. C. G. Zhan, J. A. Nichols and D. A. Dixon, *J. Phys. Chem. A*, 2003, **107**, 4184.
9. J. Muscat, A. Wander and N. M. Harrison, *Chem. Phys. Lett.*, 2001, **342**, 397.
10. B. M. W. Langeveld-Voss, R. A. J. Janssen and E. W. Meijer, J. *Mol. Struct.*, 2000, **521**, 285.
11. F. Goldoni, B. M. W. Langeveld-Voss and E. W. Meijer, *Synth. Commun.*, 1998, **28**, 2237.
12. L. S. Fuller, B. Iddon and K. A. Smith, *J. Chem. Soc., Perkin Trans. 1*, 1997, **22**, 3465.
13. P. Bonhote, E. Gogniat, S. Tingry, C. Barbe, N. Vlachopoulos, F. Lenzmann, P. Comte and M. Gratzel, *J. Phys. Chem. B*, 1998, **102**, 1498.
14. A. K. D. Diaw, A. Yassar, D. Gninngue-Sall and J. J. Aaron, *Arkivoc*, 2008, **17**, 122.
15. E. Shouji and D. A. Buttry, *Langmuir*, 1999, **15**, 669.
16. J. M. Pope, T. Sato, E. Shoji, D. A. Buttry, T. Sotomura and N. Oyama, *J. Power*

Sources, 1997, **68**, 739.

17. Y.-I. Park, J.-H. Son, J.-S. Kang, S.-K. Kim, J.-H. Lee and J.-W. Park, *Chem. Commun.*, 2008, 2143.

18. W. Fudickar and T. Linker, *Chem. Eur. J.*, 2006, **12**, 9276.

19. S. C. Dickerman, A. M. Felix and L. B. Levy, *J. Org. Chem.*, 1964, **29**, 26.

20. H. Adams, R. A. Bawa, K. G. McMillan and S. Jones, *Tetrahedron*, 2007, **18**, 1003.

21. M. Smet, J. V. Dijk and W. Dehaen, *Tetrahedron*, 1999, **55**, 7859.

22. N. Tsubokawa, M. Hosoya and J. Kurumada, *React. Funct. Polym.*, 1995, **27**, 75.

CHAPTER THREE

INVESTIGATION OF NEW THIOETHER-BASED THIOPHENES FOR PSEUDOCAPACITIVE ELECTRODES

3-1 Introduction

Previously mentioned, conducting polymers represent an attractive option as organic electrode materials for electrochemical capacitors due to their ability to store charge in a pseudocapacitive manner and their insolubility in most organic solvents used as electrolytes.[1-6] However, the capacities of these polymeric materials are low when compared to inorganic battery materials because the electrochemical reactions involve a fraction of an electron per monomer unit and the need for significant amounts of supporting electrolyte solutions lowering their gravimetric capacity and energy density.[7-9]

A substitute to conducting polymers is the use of discrete organic molecules that are capable of providing multiple electrons instead of fractional electrons, to offer high capacities and perhaps high energy/power densities with the appropriate choices.[10-15] Organic compounds promise new possibilities for high energy/power density devices, cost-effectiveness, and environmental consciousness, through low-weight and abundant elements (carbon, hydrogen, nitrogen, oxygen, sulfur, etc) and tunability, using the principles of organic chemistry. Previously, our group has studied thiophene-based organosulfur compounds (violene-type) as potential organic cathode materials for supercapacitor applications.[13] 5,5'-Bis(methylthio)-2,2'-bithiophene, BMTbT **1** (Figure 3-1) was found to be a highly promising energy storage material with the advantages of being the smallest of its kind capable of providing two chemically and electrochemically

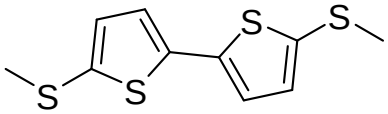

1

Figure 3-1. 5,5‘-Bis(methylthio)-2,2‘-bithiophene (BMTbT) **1**.

reversible one-electron processes at very positive potentials (3.8 and 4.0 V vs. Li/Li^+) as well as achieving a high theoretical gravimetric capacity of 209 mAh/g. Furthermore, the theoretical energy density of **1** (836 Wh/kg) is considerably larger than that of traditional inorganic battery electrode materials such as $LiFePO_4$ (495 Wh/kg) and $LiCoO_2$ (518 Wh/kg).

In designing new materials with high specific capacity, high gravimetric energy, and high power densities, three important design criteria must be considered; 1) capacity: number of electrons attainable per unit mass or volume, 2) voltage: redox potentials, and 3) stability: electrochemical and chemical reversibility. The goal is to design cathode materials that provide increased capacity, obtained from both electrochemically and chemically reversible redox processes taking place at very positive potentials (higher voltage). In the case of materials with multiple redox processes, the energy density is better when the redox potentials are closer together (smaller voltage “penalty”). The greatest asset for designing cathodes is the ability to screen promising candidates through computational efforts. Our group recently published a paper regarding computational screening of many electroactive violene-type compounds for cathode materials and pointed out several promising candidates.[16] This ability to use computational methods to screen potential candidates for their energy storage properties will facilitate the process of identifying high-energy cathode materials.

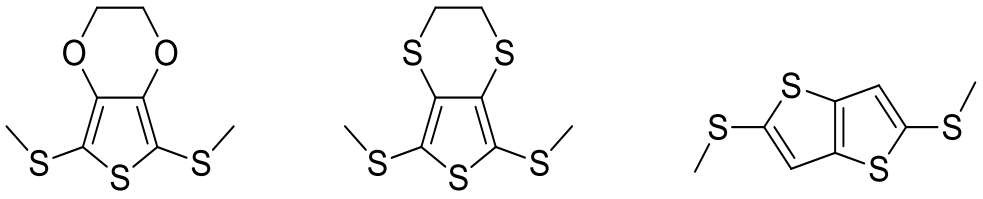

2 **3** **4**

Figure 3-2. New thiophene derivatives for potential cathode materials.

In this chapter, with the aim of identifiying new electroactive materials suitable for high power applications and using BMTbT **1** as a point of departure, three new thiophene-based organosulfur candidates (Figure 3-2) have been synthesized and electrochemically characterized. 2,5-Bis(methylthio)thieno[3,2-*b*]thiophene (FBMTbT, **4**) was thoroughly studied providing the most promise, as it affords two electrochemically and chemically reversible one-electron redox processes at potentials higher than **1**. In addition, **4** should provide higher capacity as it is lighter than **1**. Cyclic voltammetry (CV) and rotating disk electrode (RDE) voltammetry were used to evaluate the electrochemical properties of these compounds. These fundamental electrochemical evaluations are critical in the advancement of novel materials for EES applications.

3-2 Synthesis

To obtain **2** and **4**, standard dilithiation on the thiophene unit was performed using *n*-butyllithium followed by quenching with dimethyl disulfide to add the thiomethyl groups.[17] Compound **3** required multistep reactions. The first step was a substitution reaction to obtain two methoxy groups on the thiophene, and then going through an transetherification-type reaction to form the EDTT unit.[18,19] The final step involved the same type of reaction to form **2** and **4**.

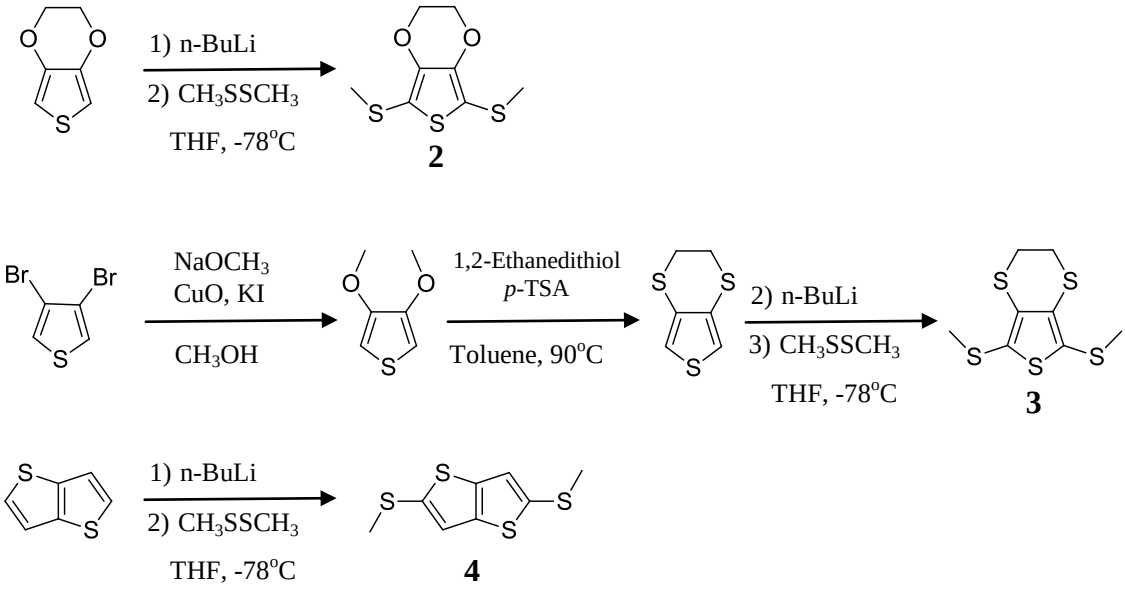

Scheme 3-1. Synthesis scheme of **2**, **3** and **4**.

3-3 Redox Behavior

a) BMT-EDOT (*2*) and BMT-EDTT (*3*)

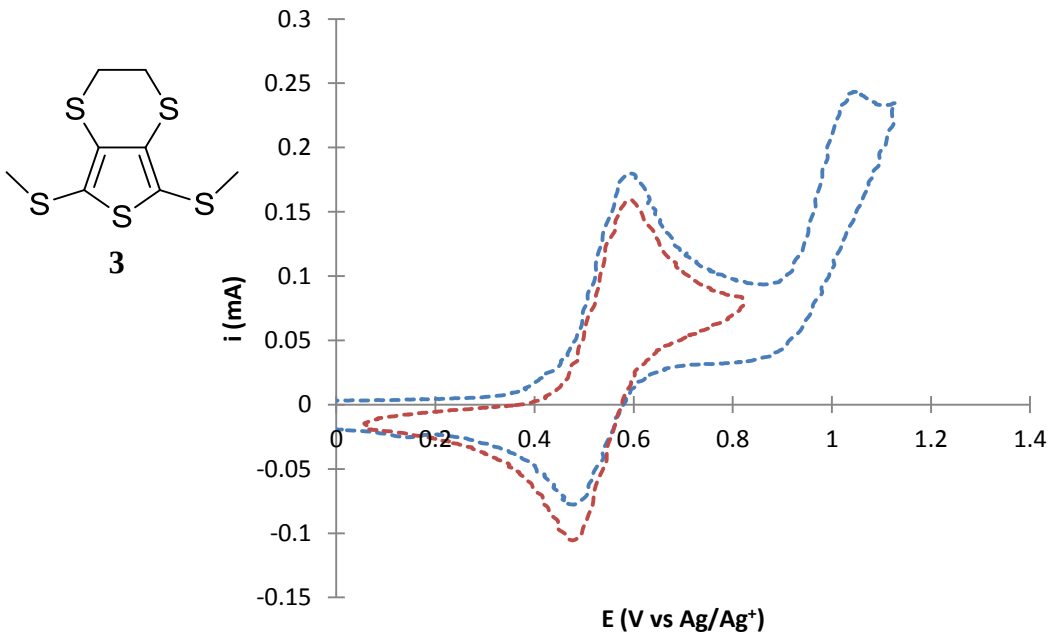

Figure 3-3. CV of 5mM **3** and 0.1M TBAH in AN, 100 mV/s.

The redox behavior of BMT-EDOT **2** is qualitatively similar to BMT-EDTT **3**.

To simplify the results, the redox behavior of BMT-EDTT **3**, via cyclic voltammetry, will be detailed here.

Figure 3-3 shows a cyclic voltammogram obtained at 100mV/s for 5mM BMT-EDTT **3** using a glassy carbon electrode in a 0.1M TBAH/AN solution. BMT-EDTT **3** exhibited two faradaic waves at formal potentials of +0.53V and +0.95V vs Ag/Ag^+ corresponding to the cation and dication, respectively. Upon switching the potential scan before the second oxidation process, the reduction of the monocation is observed. While the first redox process was shown to be chemically reversible, the second process was irreversible. Similar to **3**, only the first redox process of BMT-EDOT **2** was found to be reversible. The irreversibility on the second process is believed to arise from the undesired chemical reaction (nucleophilic attack) by the solvent or any traces of water in the electrolyte media. 2,5-Bis(methylthio)thiophene (BMTT), a similar molecule to **2** and **3**, but with no substituent groups on the 3,4 positions of thiophene, can be reversibly oxidized to the cation. Therefore, it was expected that **3** will form a stable dication due to its stabilizing electron-donating groups on the 3,4 positions. Hexaazaoctadecahydro-coronene (HOC, Figure 3-4) is a molecule saturated with alkylated amino groups around the benzene ring that can give up to four electrons reversibly (fifth electron can be observed, but slightly irreversible).[20] Similar to HOC, BMT-EDTT **3** has alkylated heteroatoms (thioethers in this case) all around the thiophene ring, anticipating that two or more electrons would be obtained, further enhancing the capacity compared to BMTbT **1**. Unfortunately, the expectation was not met as **3** only provided one electron reversibly. It was determined that both **2** and **3** did not offer a superior energy density compared to **1**.

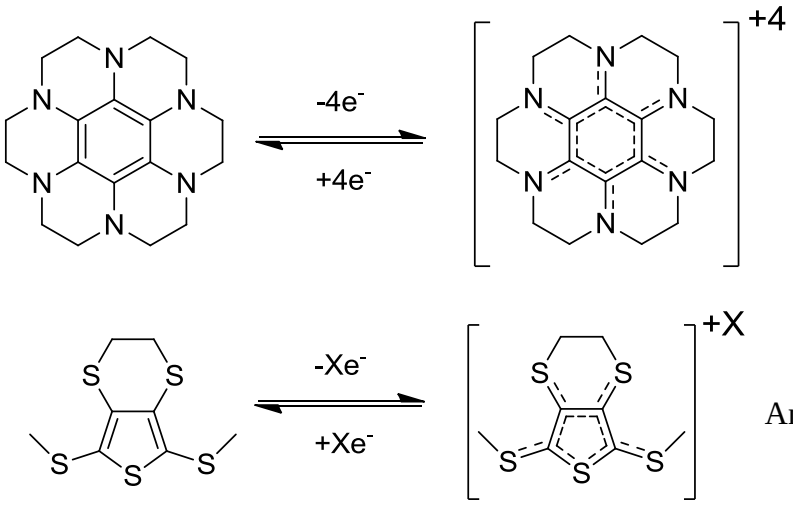

Figure 3-4. Redox properties of hexaazaoctadecahydrocoronene and **3**.

b) FBMTbT (*4*)

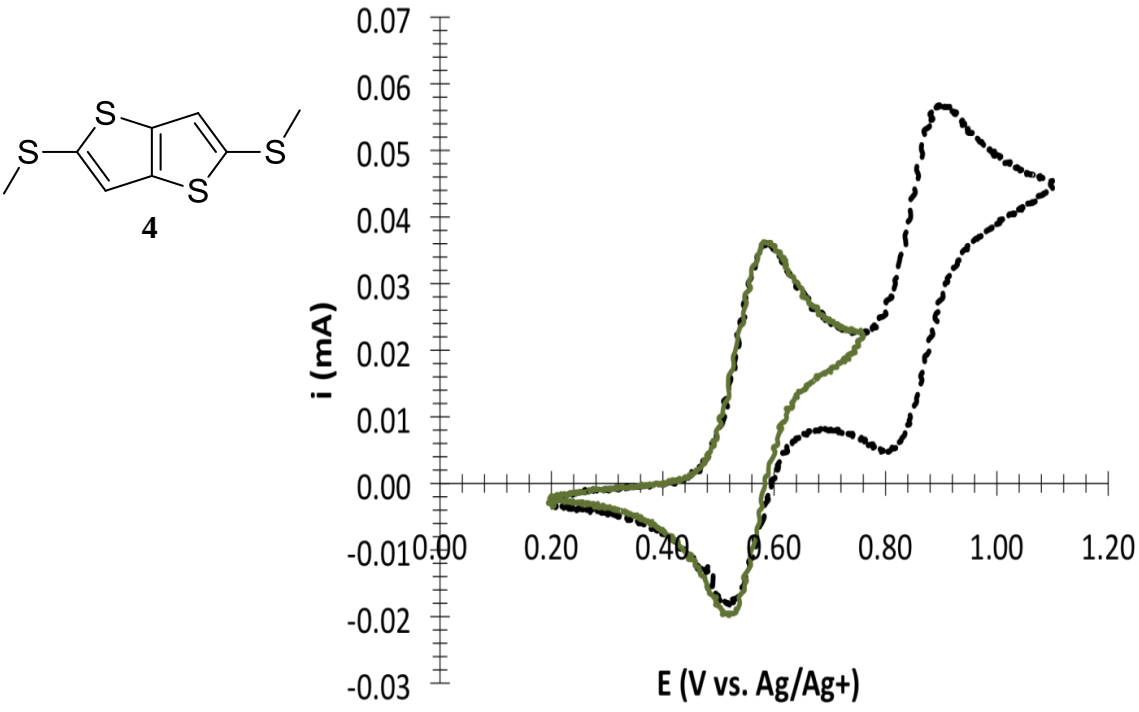

Figure 3-5. CV of 0.2mM **4** in 0.1M TBAH/AN, 20 mV/s.

Figure 3-5 shows a cyclic voltammogram obtained at 20mV/s for 0.2mM FBMTbT **4** with a glassy carbon electrode in a 0.1M TBAH/AN solution. FBMTbT **4**

displayed two redox waves at formal potentials of +0.54V and +0.87V vs Ag/Ag^+ corresponding to the cation and dication, respectively. Both of these waves in the cyclic voltammogram were chemically reversible. Scanned to the first oxidation, an intense green color was observed near the working electrode corresponding to formation of the radical cation. The two redox potentials of **4** are slightly higher than the ones for **1** due to **4** having a slightly shorter conjugation length. The stability of the dication is more affected by the conjugation length than the effect of electron donors on the 3,4 positions of thiophene (structure comparison **1**,**4** vs. **2**,**3**).

RDE experiments indicated that **4** undergoes an $E_1E_2CE_3$ or $E_1E_2C_{cat}$ mechanism overall. $E_1E_2CE_3$ represents two electrochemical steps, followed by a chemical step and then another electrochemical step. In the case of $E_1E_2C_{cat}$, two electrochemical steps are followed by a catalytic chemical step, restoring the starting material. It is expected that both E_2 and E_3 in the $E_1E_2CE_3$ mechanism will deliver a fractional electron count dependent on scan and rotation rates, totaling one electron for both steps. The RDE voltammograms in Figure 3-6a display the currents normalized to the square root of the rotation rates. Respectively, the oxidation potential of the cation and the peak currents shifted negative and increased with decreasing rotation rate. The formal potential would be expected to shift more negative when the ratio of Ox to Red is reduced. The concentration of Ox is decreased due to a following chemical step. Yet, the increased current at slow scan and rotation rates reveals that the chemical step products are oxidized at these potentials. From these observations, the mechanism was assigned as either $E_1E_2CE_3$ or $E_1E_2C_{cat}$.

Information regarding the kinetics (k_o) of the electron transfer can also be

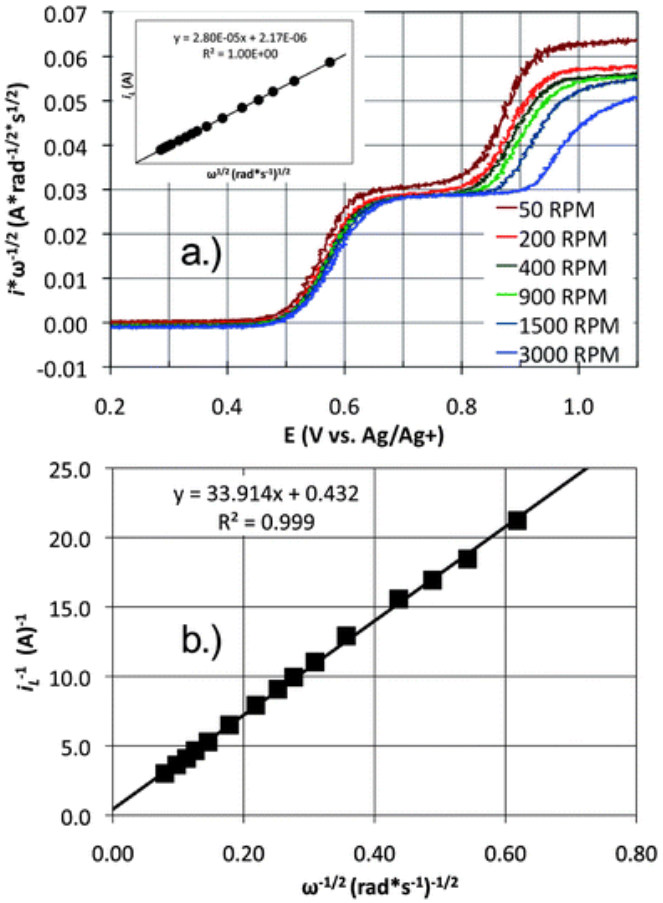

Figure 3-6. (a) RDE of 1mM **4** in 0.1M TBAH/AN at 10 mV/s, inset contains a Levich plot at 0.7 V (b) Koutecky-Levich plot at 0.62V.

obtained from the RDE data. A Levich plot (Figure 3-6a Inset) at +0.7 V of the first redox process yielded a linear curve, indicating that this process is mass transport limited at these potentials. From this, a diffusion coefficient (D_o) of 2.85 x 10^{-5} cm^2/s in acetonitrile was calculated. Analysis of the kinetically limited portion of the Koutecky–Levich data at 0.62 V afforded a heterogeneous electron transfer rate constant (k_o) of 1.4 x 10^{-2} cm/s, which is comparable to BMTbT **1** and places the first redox couple in the range of an electrochemically reversible reaction. The value of k_o indicates that the kinetic facility of the first redox process of **4** can achieve the high rates applicable to devices based on pseudocapacitive electrodes.

3-4 Summary & Conclusions

Compound	BMTbT 1	FBMTbT 4	$LiCoO_2$	$LiFePO_4$
Capacity (Ah/kg)	209	232	140	150
V_1 (V vs Li/Li^+)	3.8	3.8	3.7	3.3
V_2 (V vs Li/Li^+)	4.0	4.2	-	-
Energy Density (Wh/kg)	836	974	518	495

Table 3-1. Cathode materials and properties.

Electrochemical results suggest that FBMTbT **4** is an excellent material for high-energy and high-power cathode due to its light weight with multiple reversible redox processes. RDE experiments confirmed that the kinetic facility of **4** can achieve the rates relevant to devices based on pseudocapacitive electrodes. As shown in Table 3-1, **4** has shown an improvement in the energy density compared to BMTbT **1** by 138Wh/kg and is approximately twice that of traditional inorganic battery materials such as $LiCoO_2$ and $LiFePO_4$. In the future, hexaazaoctadecahydrocoronene and similar molecules should also be studied as cathode materials due to their potentially high capacity (up to two or more exchangeable electrons). In conjunction with computational methods, a systematic study of the influence of heteroatoms and aromatic rings on stability and redox potentials of electroactive compounds should also be investigated. Future studies should also include stability dependence with electrolyte media (different solvent and salt combinations). These investigations will facilitate the design process for the next generation high energy cathode materials.

As promising as these discrete organic compounds appear to be, there are several disadvantages: the high solubility in organic solvents that results in a rapid fade in the capacity and the need for adding a conducting additive since organic materials are usually insulators. The next chapter will focus on addressing these limitations of these small organics through the utilization of a 'hybrid' approach (Figure 1-8) by employing another highly promising material, *N*,*N*,*N*′,*N*′-tetramethyl-*p*-phenylenediamine (TMPD).

3-5 References

S. E. Burkhardt, S. Conte, G. G. Rodriguez-Calero, M. A. Lowe, H. Qian, W. Zhou, J. Gao, R. G. Hennig and H. D. Abruña, *J. Mater. Chem.*, 2011, **21**, 9553.

Reproduced by permission of The Royal Society of Chemistry.

http://pubs.rsc.org/en/content/articlelanding/2011/jm/c1jm10664c

1. P. Simon and Y. Gogotsi, *Nat. Mater.*, 2008, **7**, 845.
2. G. A. Snook, P. Kao and A. S. Best, *J. Power Sources*, 2011, **196**, 1.
3. G. Wang, L. Zhang and J. Zhang, *Chem. Soc. Rev.*, 2012, **41**, 797.
4. A. Burke, *J. Power Sources*, 2000, **91**, 37.
5. M. Mastragostino, C. Arbizzani and F. Soavi, *J. Power Sources*, 2001, **97-98**, 812.
6. K. Gurunathan, A. V. Murugan, R. Marimuthu, U. P. Mulik and D. P. Amalnerkar, *Mater. Chem. Phys.*, 1999, **61**, 173.
7. M. Mastragostino, C. Arbizzani and F. Soavi, *Solid State Ionics*, 2002, **148**, 493.
8. P. Novak, K. Muller, K. S. V. Santhanam and O. Haas, *Chem. Rev.*, 1997, **97**, 207.
9. G. Zotti, S. Zecchin and G. Schiavon, *Chem. Mater.*, 2000, **12**, 2996.

10. Y. Liang, Z. Tao and J. Chen, *Adv. Energy Mater.*, 2012, ***2***, 742.

11. Y. Kiya, J. C. Henderson, G. R. Hutchison and H. D. Abruña, *J. Mater. Chem.*, 2007, **17**, 4366.

12. Y. Kiya, J. C. Henderson and H. D. Abruña, *J. Electrochem. Soc.*, 2007, **154**, A844.

13. J. C. Henderson, Y. Kiya, G. R. Hutchison and H. D. Abruña, *J. Phys. Chem. C*, 2008, **112**, 3989.

14. S. E. Burkhardt, S. Conte, G. G. Rodriguez-Calero, M. A. Lowe, H. Qian, W. Zhou, J. Gao, R. G. Hennig and H. D. Abruña, *J. Mater. Chem.*, 2011, **21**, 9553.

15. S. Conte, G. G. Rodriguez-Calero, S. E. Burkhardt, M. A. Lowe and H. D. Abruña, *RSC Adv.*, 2013, **3**, 1957.

16. S. E. Burkhardt, M. A. Lowe, S. Conte, W. Zhou, H. Qian, G. G. Rodriguez-Calero, J. Gao, R. G. Hennig and H. D. Abruña, *Energy Environ. Sci.*, 2012, **5**, 7176.

17. L. S. Fuller, B. Iddon and K. A. Smith, *J. Chem. Soc., Perkin Trans. 1*, 1997, **22**, 3465.

18. B. M. W. Langeveld-Voss, R. A. J. Janssen and E. W. Meijer, J. *Mol. Struct.*, 2000, **521**, 285.

19. F. Goldoni, B. M. W. Langeveld-Voss and E. W. Meijer, *Synth. Commun.*, 1998, **28**, 2237.

20. J. S. Miller, D. A. Dixon, J. C. Calabrese, C. Vazquez, P. J. Krusic, M. D. Ward, E. Wasserman and R. L. Harlow, *J. Am. Chem. Soc.*, 1990, **112**, 381.

CHAPTER FOUR

DESIGNING CONDUCTING POLYMER FILMS FOR ELECTROCHEMICAL ENERGY STORAGE TECHNOLOGIES

4-1 Introduction

Rapid advances in the design of electroactive materials for electrical energy storage (EES) devices have yielded several promising organic systems suitable for high energy/power applications. Currently, research in electrode materials for electrochemical capacitors has focused on high surface area carbons (HSAC) and metal oxides such as RuO_2.[1-6] While these materials can sustain high charge/discharge rates, they are offset by low capacities in the case of HSAC and high costs in the case of metal oxides. Conducting polymers (CP) have also been studied as materials for EES applications. These, however, suffer from low capacities due to the fractional electrons obtainable from the monomer units of the polymer.[7-9] An alternative would be the use of discrete organic molecules, capable of exchanging multiple electrons, yielding high capacity, and if the proper choice is made, also high energy and power density.[10-14] However, these small organics have several shortcomings: high solubility in organic solvents (even higher for their oxidized, cationic species) that translates to a rapid fade in the capacity of the EES device, and the need for adding a conducting additive (e.g. carbon black) since such molecules are generally insulators.

Based on these constraints, we decided to develop 'hybrid' type materials composed of redox-active organics anchored to conductive polymer backbones. These 'hybrid' composite materials address the shortcomings of both CPs and discrete small

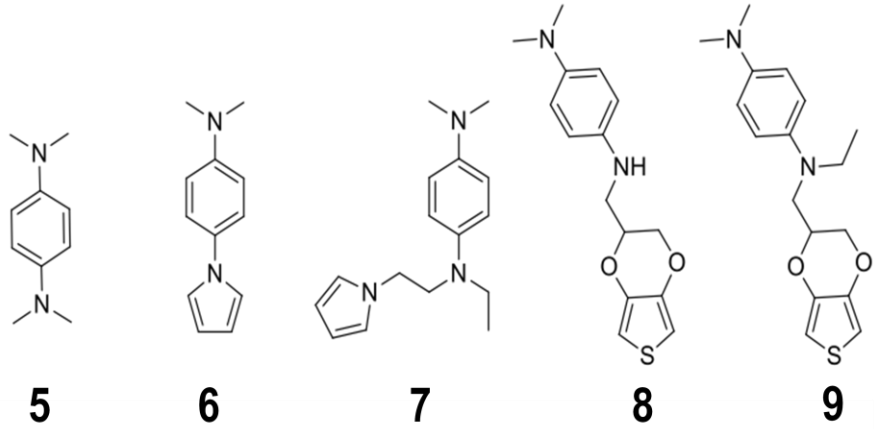

Figure 4-1. Chemical structures of the hybrid electro-active monomer. (**5**) N,N,N',N'-Tetramethyl-*p*-phenyldiamine (TMPD), (**6**) 1-(4-dimethylamino)pyrrole, (**7**) *N*-(2-(1*H*-pyrrol-1-yl)ethyl)-*N*-ethyl-*N',N'*-dimethyl-*p*-phenylenediamine, (**8)** *N*-((2,3-dihydrothieno[3,4-b][1,4]dioxin-2-yl)methyl)-*N',N'*-dimethyl-*p*-phenylenediamine, (**9**) *N*-((2,3-dihydrothieno[3,4-b][1,4]dioxin-2-yl)methyl)-*N*-ethyl-*N*',*N*'-dimethyl-*p*-phenylenediamine.

redox-active organic molecules (i.e. low capacities for CPs and solubility in the electrolyte solution for small organic molecules). We recently demonstrated the feasibility of this approach by synthesizing a 'hybrid' material with redox-active 5,5' -bis(methylthio)-2,2'-bithiophene (BMTbT) as a pendant to an insoluble conducting poly(3,4-ethylenedioxythiophene) (PEDOT) backbone, for its use as a positive electrode (cathode) material in supercapacitor applications.[15] In addition, there are other examples in the literature of analogous materials being used as electrode materials.[16-18]

Using the results from the PEDOT-BMTbT system as a point of departure, we have designed a family of 'hybrid' materials using *N*,*N*,*N'*,*N'*-Tetraalkylated-*p*-phenylenediamine (TAPD) as a redox-active pendant. *N*,*N*,*N'*,*N'*-Tetramethyl-*p*-phenylenediamine (TMPD) **5** can be oxidized to form the well-known stable cation known as "Wurster's Blue", which can be further oxidized to form the quinonediiminium dication.[19-21] To the best of our knowledge, this is the first attempt to use TMPD as an EES electrode material. TMPD's appeal as an EES electrode material derives from its

reversible two-electron electrochemistry at high potentials and its low molecular weight, which yield a high capacity and high energy density material. Yet, similar to most other small organics, TMPD suffers from high solubility and low conductivity. To mitigate these aspects, a family of potentially electropolymerizable 'hybrid' monomers was synthesized (Figure 4-1) and their electrochemical properties were investigated for their potential use as cathode materials for EES applications. These 'hybrid' materials are also more promising than the previous generation of EDOT-BMTbT system because their synthesis is simpler. The synthetic strategy, chemical analysis, electropolymerization, and film electrochemistry are presented and discussed below.

4-2 Synthesis Pathway and Design Criteria

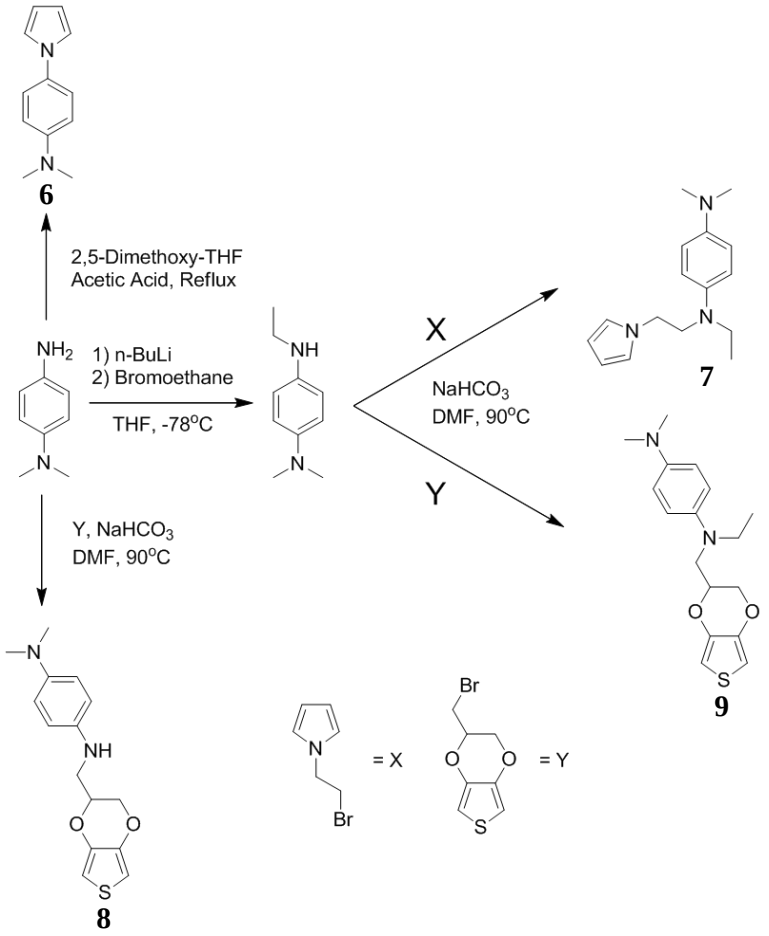

Scheme 4-1. Synthesis scheme of hybrid monomers **6**, **7**, **8**, and **9**.

The following synthetic strategy was taken. First, we attempted to synthesize a very simple TMPD-like compound that could potentially be electropolymerized. Thus **6** was synthesized by forming a pyrrole group using the free amine on *N*,*N*-dimethyl-*p*-phenylenediamine via Clauson-Kaas pyrrole synthesis. Following electrochemical results from **6** (next section), monomer **7** was prepared in order to separate the pendant from the pyrrole unit since we felt that if the electropolymerizable monomer was too close to its redox-active pendant, it could inhibit electropolymerization.

Using our previous knowledge of the EDOT-BMTbT 'hybrid' using EDOT as the polymerizable unit, monomers **8** and **9** were prepared. Monomer **8** is essentially identical to **9**, but without an ethyl group attached to one of the amines. This was interesting because **8** required fewer synthetic steps and has a lower molecular weight (higher capacity) compared to **9**.

4-3 Cyclic Voltammetry Experiments of Monomers in Solution

MONOMER	5	6	7	8	9	$LiCoO_2$
Scanning Potential Range (E_1, E_2) / (V)	N/A	(1.50, -0.45)	(1.50, -0.50)	(1.10, -0.50)	(1.10, -0.50)	N/A
Redox Pendant Formal Potentials ($E^{0'}_1$, $E^{0'}_2$) / (V)	(-0.23, 0.36)	(0.41)	(-0.19, 0.40)	(-0.15, 0.45)	(-0.17, 0.44)	N/A
Monomer Oxidation Onset Potential (E_{ons}) / (V)	N/A	N/A	N/A	(0.95)	(1.0)	N/A
Film Formation	N/A	No	No	Yes	Yes	N/A
Cyclability of CP Film	N/A	N/A	N/A	Fair	Good	N/A
Theoretical Capacity for a 2, 2.6, 2.6, 2.6, and 1 e^- processes respectively (mAh/g)	(327)	(288)	(271)	(229)	(210)	(273)

Table 4-1. Electrochemical parameters and its values for the molecules under study.

Films of the electroactive pendant CP 'hybrid' films were prepared via anodic electropolymerization using CV. Depending on the monomer under study, different switching potentials were chosen in order to favor CP film formation onto the GCE. The electropolymerization conditions and results for monomers **6**, **7**, **8**, and **9** are presented in

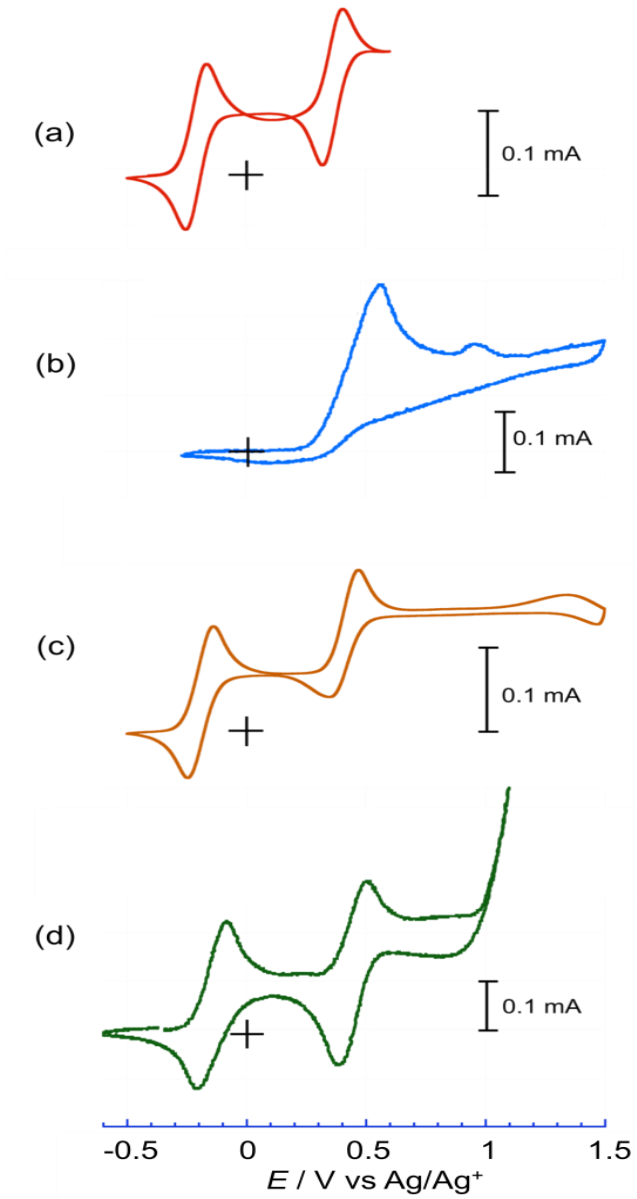

Figure 4-2. Representative CVs (first cycles) of monomers **5** (10 mM), **6** (10 mM), **7** (10 mM), and **8** (10 mM) in 0.1 M TBAP/AN solutions at a sweep rate of 20 mV/s.

Table 4-1. First CV cycles of the monomers under study are presented in Figure 4-2. It can be seen that monomers **6** and **7** did not form electroactive CP films on the electrode surface using the listed conditions. This is evident because even at high overpotentials, the oxidation of the CP backbone is not apparent. TMPD **5** is the pendant unit that was being coupled to the five-membered heterocyclic ring. This molecule has been well studied in the literature and we report the formal potentials for the first and second oxidations as -0.23 and 0.36 V, respectively, as presented in Table 4-1 and Figure 4-2a. Monomer **6** was synthesized in an effort to retain most of the capacity of **5** by using a molecule with minimal additional weight. Despite many attempts under a broad range of conditions there was no evidence of CP film formation (Figure 4-2b). We reasoned that the close proximity between the pendant and the polymerizable group precluded film formation. Taking this into account, we then proceeded to separate the redox-active pendant from the five membered heterocycle in an effort to minimize such deactivating interactions. In order to achieve this, monomer **7** was synthesized. This material exhibited two anodic redox processes with formal potentials at -0.19 and 0.40 V, respectively, but again no film formation was observed during cycling up to 1.5 V (Figure 4-2c).

Our unsuccessful attempts at electropolymerizing monomers **6** and **7** suggested that pyrrole rings might not yield electroactive CP films when covalently bound to **5** as a pendant. In order to test for this, a different monomer unit was chosen: 3,4-ethylenedioxythiophene (EDOT). Electropolymerization attempts using EDOT units as the five-membered heterocycle covalently bound to electroactive pendants has been previously reported by our group for EDOT-BMTbT monomer.[14] For this reason we synthesized monomers **8** and **9** and found that both yielded electroactive films on GCEs

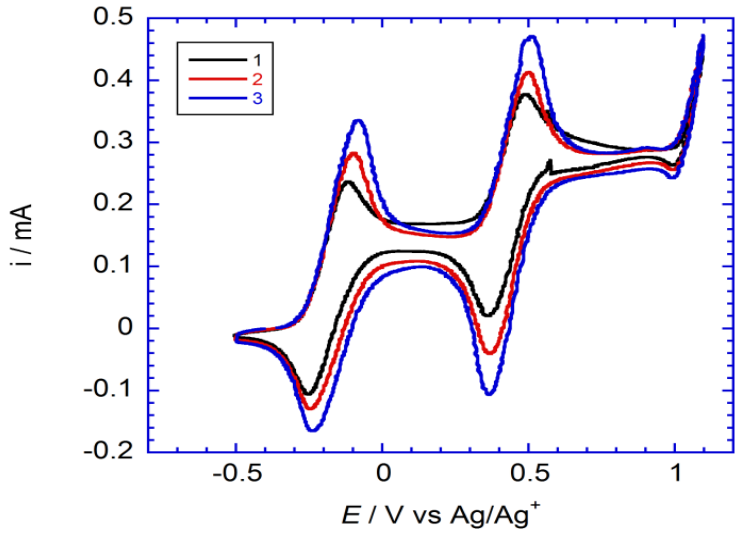

Figure 4-3. Representative CV of the electropolymerization of 20 mM monomer **9** in 0.1 M TBAP/AN at a sweep rate of 20 mV/s.

upon consecutive cycling as evidenced by EDOT oxidation after the two redox waves of TAPD.

Consecutive cyclic voltammograms for monomer **9** are presented in Figure 4-3, in which potential cycling between -0.5 to 1.1 V was carried out. During such consecutive potential cycling, the peak current, as well as the double layer capacitance increased, evidencing formation of a CP film on the electrode surface. The anodic peaks at -0.10 and 0.50 V correspond to the oxidation of the TAPD pendant from the neutral species to the cation and dication species, respectively. The most positive oxidation wave, with an onset potential of about 1.0 V is due to the oxidation of the EDOT backbone. The oxidation onset potential for EDOT, under similar conditions, is more negative than that for monomer **9**. However the shift towards positive values is expected due to the 2+ charge on the pendant group so that further oxidation (to a 3+ ion) would be energetically unfavorable. The reverse (cathodic) sweep exhibits two main reduction waves at -0.23 and 0.37 V corresponding to the reduction of the pendant TAPD cation to the neutral and

dication to the cation, respectively. There is a small oxidation wave at 0.9 V and a reduction wave at 1.0 V in the electropolymerization CVs, but we are uncertain as to their origin. Results for the electropolymerization of monomer **8** are qualitatively similar to those of monomer **9** and the data are presented in Table 4-1. The first cycle CV of this monomer **8** is presented in Figure 4-2d. It is important to note that all of these materials have a higher theoretical capacity than $LiCoO_2$; the cathode battery electrode material of choice in current lithium ion batteries, while exhibiting much higher rate capabilities as will be discussed below.

4-4 Electrochemistry of Electroactive Films

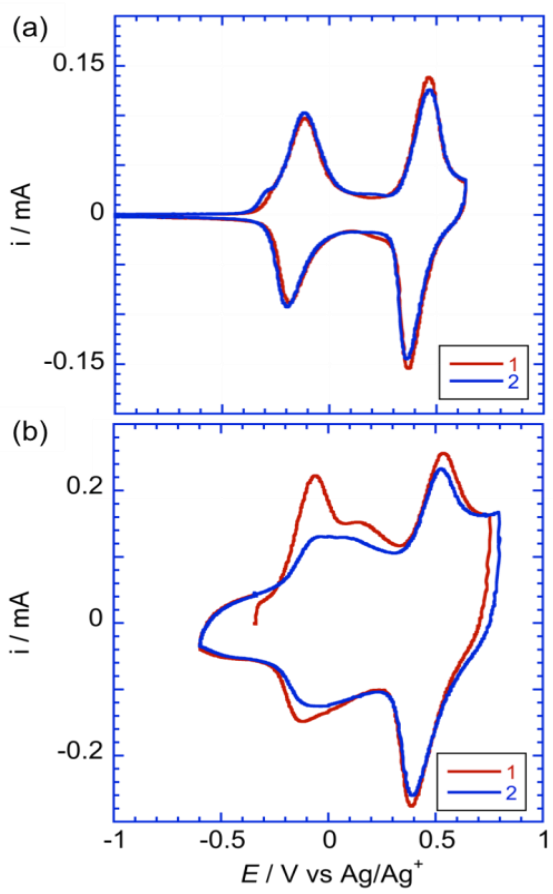

Figure 4-4. Representative CV of the first two cycles for the CP film-modified GCEs of (a) poly-**9**, and (b) poly-**8** at a sweep rate of 20 mV/s.

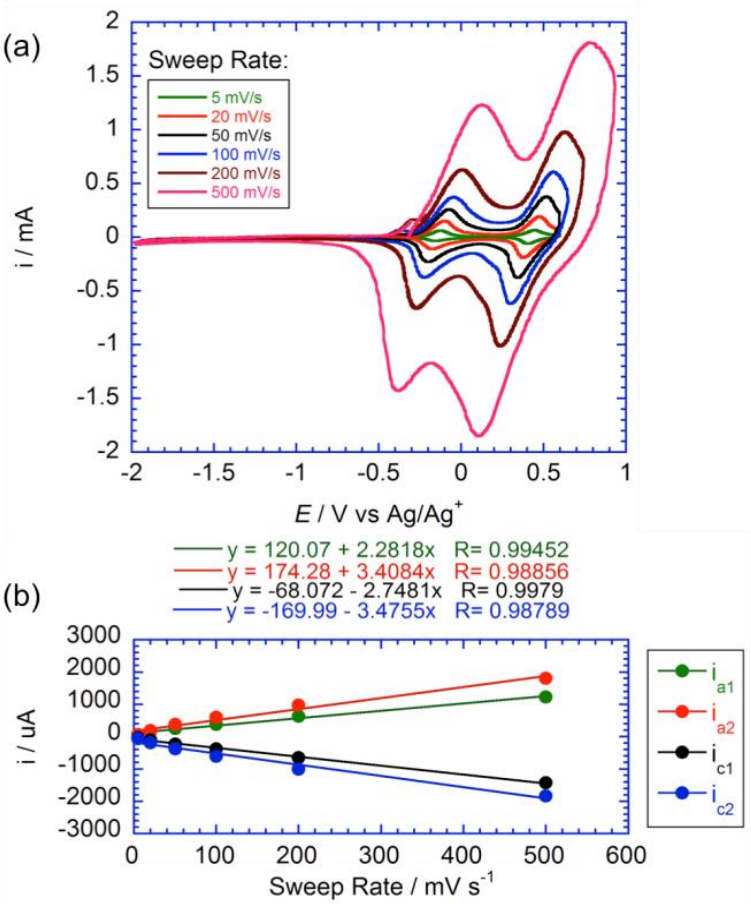

Figure 4-5. (a) Sweep rate dependent CVs and (b) Peak current vs sweep rate plot for a polymer **9** film-modified GCE.

The CV properties at 20 mV/s for the electrochemically active CP films are shown in Figure 4-4. It can be observed that the CP films corresponding to monomer **8** and **9** exhibit contributions from both the CP backbone, as evidenced by the pseudocapacitive nature of the background, and from the pendant, as exibited by the surface redox waves corresponding to TAPD; at potentials that correspond to the generation of the cation and dication, respectively. Figure 4-5 shows the sweep rate dependence of the electrochemical activity of a film of poly-**9**. The poly-**9** film exhibits two faradaic waves at formal potentials of -0.25 and +0.45 V corresponding to the cation and dication, respectively (Figure 4-4a). In addition, the current was directly proportional

to the sweep rate as anticipated for a surface-confined redox process. It is also evident that there is an increase in the peak-to-peak potential separation (ΔE_p) with sweep rate and this is most likely due to film resistance. The electrochemical and chemical cyclability (stability) for this film were good, as evidenced by the steady state response of the film during continuous electrochemical cycling.

Monomer **8** could also be electropolymerized to yield an electroactive film. This CP film exhibited two oxidation processes with formal potentials at -0.15 and 0.50 V as shown in Figure 4-4b. The electrochemical and chemical stability of the film upon cycling were not as good as for films of poly-**9**, as evidenced by the diminution of the surface waves from the first to the second cycle. We believe the poor cycling is due to the reactivity of the secondary-amine on the pendant since the pseudocapacitive response is preserved and because films of poly-**9**, that contain a tertiary-amine, are more stable, as mentioned above. The electrochemical cycling at 500 mV/s shows that the peak current retention is above 90% for 25 cycles (Figure 4-6). Having such electrochemical stability at these extremely high rates (i.e. over 1000 C) illustrates the promise of these type of electrode materials for EES devices.

For monomers **6** and **7**, film formation was not observed as mentioned in the previous section. These monomers would make polymeric materials with higher energy densities and higher capacities than the PEDOT based CP 'hybrids', **8** and **9**, due to their lower mass. For monomers **6** and **7**, different strategies will be needed to deposit CP films. These strategies could include the use of different electrolyte media, or starting from dimers of **6** and **7,** instead of the monomers (increasing the conjugation length, therefore decreasing the onset potential of the pendant oxidation). Such studies are

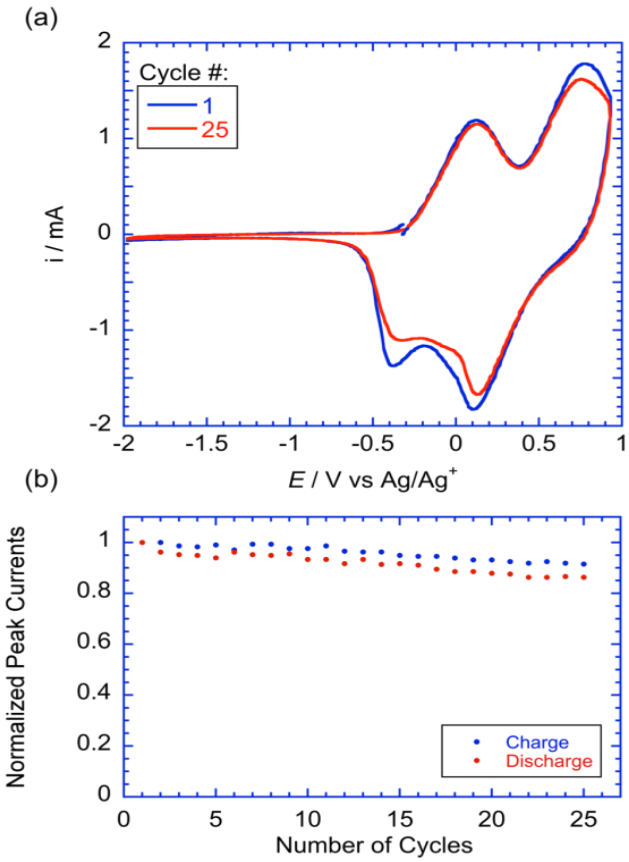

Figure 4-6. (a) Electrochemical cycling of polymer **9** film-modified GCE at 500 mV/s, and (b) normalized peak current vs. number of cycles.

currently underway.

4-5 Computational Studies

Following experimental studies, a computational investigation was undertaken with the intent of confirming the nature of the observed oxidations and providing insight into possible reasons for the differing film formation characteristics of monomers **6-9**.

The oxidations potentials for **6-9** were computed in order to support the validity of arguments based on computational data. As can be seen in Figure 4-7, there is a strong correlation between computed and observed electrochemical results. This suggests that the ground state properties of both neutral and oxidized forms are well converged at this

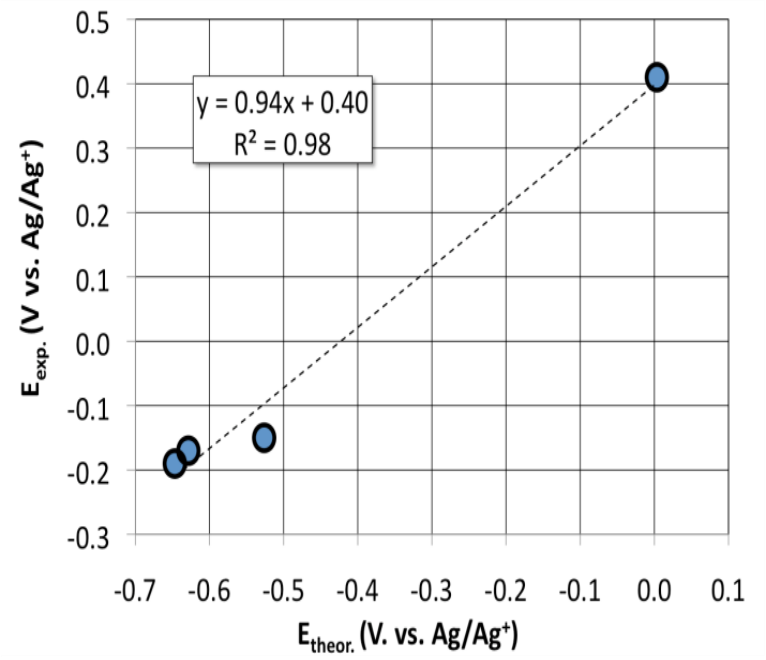

Figure 4-7. Calculated oxidation potentials for **6**-**9** vs. the observed first oxidation. The high correlation suggests that the ground state properties of both neutral and oxidized forms are well described at this level of theory.

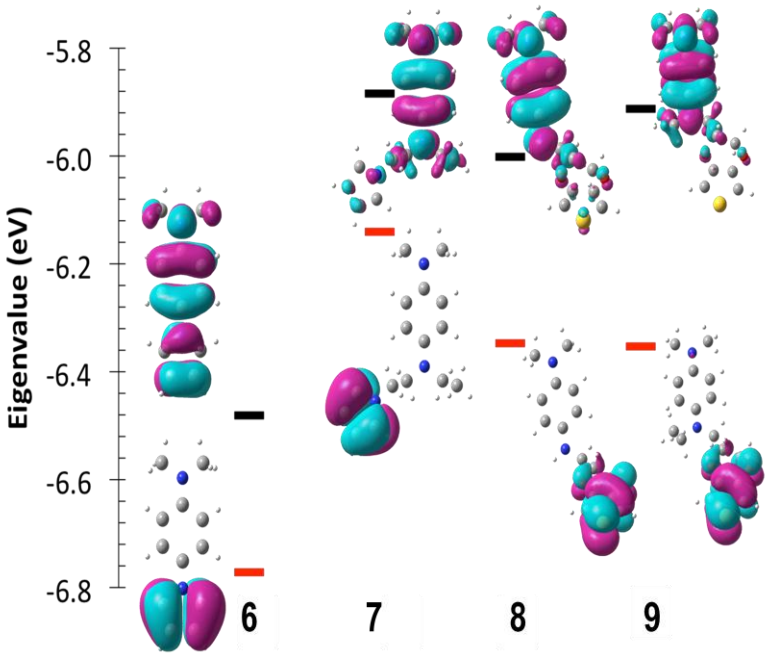

Figure 4-8. SOMO and SOMO-1 eigenvalues and isosurfaces for **6-9**. Isosurfaces are in agreement with the assumptions for film preparation (that the third oxidation leads to film formation). SOMO and SOMO-1 levels also suggest that **6** will be difficult to polymerize due to very positive oxidations.

level of theory.

Based on the agreement shown in Figure 4-7, a series of isosurfaces for the oxidized species were prepared with the intent of identifying the nature of successive oxidations, and verifying the underlying principles for electropolymerization. The rendered isosurfaces include the singly occupied molecular orbital (SOMO) and the next lowest energy orbital (SOMO-1), which are shown in Figure 4-8. Rather than the neutral molecule, the orbitals of the oxidized molecule (SOMO, SOMO-1) were chosen due to the possibility of differing geometries and electronic relaxation effects following oxidation. These surfaces demonstrate, with clarity, that the underlying principles for electropolymerization of these materials, which state that the first two oxidations should be associated with the pendant and the third associated with the monomeric component, are correct.

As can be seen in Figure 4-8, the SOMO is clearly TAPD-pendant in nature for species **7-9**, with the SOMO-1 being largely centered on the monomeric component (EDOT and pyrrole, in this case). The exception to this is **6**, which shows a heavily delocalized SOMO, further supporting previous assertions in this report that charge is delocalized across both phenyl and pyrrole units in the radical cation. Also apparent is the significant negative shift of the SOMO for **6**. This observed shift, when combined with the observation of only a single redox process at potentials positive of those for **7-9**, indicates that the alkyl-amine moiety of the pyrrole ring is clearly not electron-donating as in **5**. The lack of electron donation in **6** is likely responsible for the positive shift in the first oxidation and the difficulty in accessing subsequent oxidations. However, the calculated SOMO-1 of **6** is clearly pyrrole in nature.

4-6 Conclusions

We have demonstrated the synthesis and the characterization of hybrid materials for potential applications in electrochemical energy storage devices containing a discrete pendant TAPD group along with electropolymerizable pyrrole and EDOT units. We have characterized all the materials and found that only those containing EDOT could be electropolymerized. In addition the nature of the resulting film was strongly dependent on the presence of amine hydrogens. The electropolymerized film exhibited contributions from both the conducting polymer backbone and the pendant groups.

From computational studies, the concepts of film preparation were verified, as well as the sequence of oxidations. However, in the case of **6**, electrochemical and computational methods indicate that the pyrrole moiety does not result in significant electron donation to the TAPD and shifts the oxidation to much more positive potentials. Electronic communication between pendant and backbone was found to play an important role for the electropolymerization reaction; where greater delocalization across monomer and pendant seems to inhibit the electropolymerization reaction. These materials appear to be promising candidates for EES application and serve to illustrate the potential of organic systems for such applications.

4-7 References

S. Conte, G. G. Rodriguez-Calero, S. E. Burkhardt, M. A. Lowe and H. D. Abruña, *RSC Adv.*, 2013, **3**, 1957.

1. E. Frackowiak and F. Beguin, *Carbon,* 2001, **39**, 937.

2. P. Simon and Y. Gogotsi, *Nat. Mater.*, 2008, **7**, 845.

3. C. Arbizzani, M. Mastragostino and F. Soavi, *J. Power Sources*, 2001, **100**, 164.

4. B. E. Conway, V. Birss and J. Wojtowicz, *J. Power Sources*, 1997, **66**, 1.

5. B. E. Conway, *Electrochemical Supercapacitors-Scientific Fundamentals and Technological Applications*, Kluwer Academic: New York, 1999.

6. D. Galizzioli, F. Tantardini and S. Trasatti, *J. Appl. Electrochem.*, 1974, **4**, 57.

7. M. Mastragostino, C. Arbizzani and F. Soavi, *Solid State Ionics*, 2002, **148**, 493.

8. P. Novak, K. Muller, K. S. V. Santhanam and O. Haas, *Chem. Rev.*, 1997, **97**, 207.

9. G. Zotti, S. Zecchin and G. Schiavon, *Chem. Mater.*, 2000, **12**, 2996.

10. Y. Liang, Z. Tao and J. Chen, *Adv. Energy Mater.*, 2012, **2**, 742.

11. Y. Kiya, J. C. Henderson, G. R. Hutchison and H. D. Abruña, *J. Mater. Chem.*, 2007, **17**, 4366.

12. Y. Kiya, J. C. Henderson and H. D. Abruña, *J. Electrochem. Soc.*, 2007, **154**, A844.

13. J. C. Henderson, Y. Kiya, G. R. Hutchison and H. D. Abruña, *J. Phys. Chem. C*, 2008, **112**, 3989.

14. S. E. Burkhardt, S. Conte, G. G. Rodriguez-Calero, M. A. Lowe, H. Qian, W. Zhou, J. Gao, R. G. Hennig and H. D. Abruña, *J. Mater. Chem.*, 2011, **21**, 9553.

15. M. A. Lowe, Y. Kiya, J. C. Henderson and H. D. Abruña, *Electrochem. Commun.*, 2011, **13**, 462.

16. M. Aydin, B. Esat, C. Kilic, M. E. Kose, A. Ata and F. Yilmaz, *Eur. Polym. J.*, 2011, **47**, 2283.

17. T. K. Kunz and M. O. Wolf, *Polym. Chem.*, 2011, **2**, 640.

18. K.-S. Park, S. B. Schougaard and J. B. Goodenough, *Adv. Mater.* 2007, **19**, 848.

19. A. Ito, D. Sakamaki, H. Ino, A. Taniguchi, Y. Hirao, K. Tanaka, K. Kanemoto and T. Kato, *Eur. J. Org. Chem.*, 2009, **26**, 4441.

20. M. Morimoto, S. Kobatake and M. Irie, *Chem. Commun.*, 2006, **25**, 2656.

21. L. Michaelis, M. P. Schubert and S. Granick, *J. Am. Chem. Soc.*, 1939, **61**, 1981.

CHAPTER FIVE

ELECTROCHEMICAL CHARACTERIZATION & DEVICE TESTING OF POLY-(EDOT-TAPD) FILM

5-1 Introduction

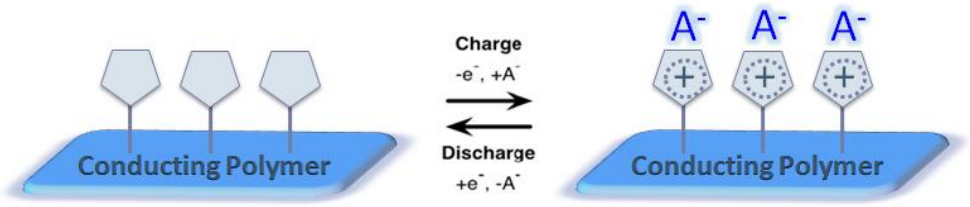

Figure 5-1. Schematic depiction of the 'hybrid' approach.

Conducting polymers represent one class of electrode materials receiving increased attention due to their potential in meeting demands for both high energy and high power applications in electrical energy storage (EES). As mentioned in Chapter 1, a 'hybrid' approach (Figures 1-8 and 5-1) is one plausible means to enhance capacity, and in turn, energy density. Chemically anchoring electroactive pendant additives onto a conducting polymer can improve the capacity by increasing the charge to weight ratio. As the use of 'hybrid' materials as electrode materials is almost none existent in the literature, the application of these novel materials can play a crucial role in current and emerging electrical energy storage technologies, competing and surpassing traditional electrode materials.

In Chapter 4, a family of 'hybrid' monomers containing a discrete pendant *p*-phenylenediamine group along with electropolymerizable pyrrole and EDOT units were synthesized and characterized for potential applications in EES devices. Continuing the

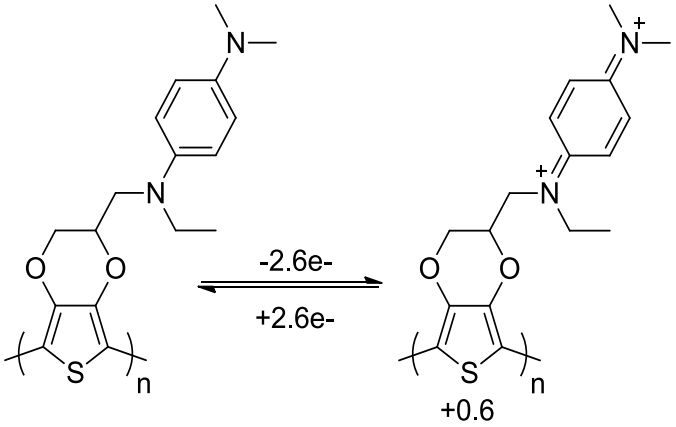

Figure 5-2. Redox property of poly-**9**.

efforts, this chapter specifically focuses on additional electrochemical characterization and device testing of the 'hybrid' polymer produced from **9**. The 'hybrid' monomer **9** is electropolymerized, ostensibly through the EDOT units, to yield a poly-3,4-ethylenedioxythiophene (PEDOT)/*N*,*N*,*N*′,*N*′-Tetraalkylated-*p*-phenylenediamine (TAPD) composite films (poly-**9** or poly-(EDOT-TAPD)**,** Figure 5-2) capable of storing up to 2.6 electrons per monomer unit with contributions from both the conducting polymer (pseudocapacitance, ca 0.6 electron) and the organic pendant (faradaic, two electrons). Similar to *N*,*N*,*N*′,*N*′-tetramethyl-*p*-phenylenediamine (TMPD) **5**, the pendant group on poly-**9** can be oxidized to form a stable cation like the "Wurster's Blue". [1-3] Further oxidation by a second electron yields the quinonediiminium dication. Poly-**9** is a highly promising material as evidenced by its high theoretical capacity (220 mAh/g) and its stable film electrochemistry (Figure 4-6). The electrochemical cycling at 500 mV/s shows that the peak current retention is above 90% for 25 cycles, demonstrating its promise as an electrode material for EES devices. The results showed that anchored pendants are electrochemically active and stable, and the connection between EDOT and TAPD is short enough to ensure an electronic conduction pathway for TAPD.

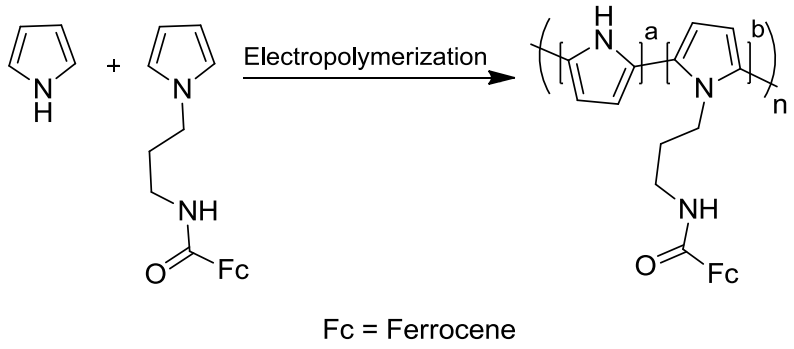

Figure 5-3. Co-electropolymerization of pyrrole and ferrocene-functionalized pyrrole.

The major obstacle faced initially was the inability to make a bulk material of poly-**9** for device testing. Only one example of oxidative chemical polymerization of a 'hybrid' material (polythiophene/TEMPO composite) was found in the literature.[4] Similar reaction conditions were applied for monomer **9**, but the synthesis of its polymer was unsuccessful. This can be attributed to the fact that poly-**9** has a pendant group that forms a dication instead of a cation, which can complicate the reaction (forming only short-chain soluble oligomers or by-products from side-reactions due to higher reactivity of the dication). Different oxidative chemical polymerization conditions were attempted multiple times ($FeCl_3$ in $CHCl_3$, CH_3NO_2, or CH_3NO_2-CCl_4 and n-BuLi/$CuCl_2$ in THF), but unsuccessful results followed.

After the failed chemical synthesis of poly-**9**, a different methodology was searched throughout the literature. The method that was established was electro-polymerizing hybrid-type materials directly onto a current collector. Goodenough et al. demonstrated the feasibility of the electrosynthesis of 'hybrid' polymers for battery application by co-electropolymerizing pyrrole and ferrocene-anchored pyrrole to form a polypyrrole (PPy)/ferrocene composite polymer onto a stainless-steel mesh (Figure 5-3).[5] From the charge–discharge curves, PPy/ferrocene film exhibited a capacity of 65 mAh/g

with a short voltage plateau near 3.5 V vs Li^+/Li corresponding to the ferrocene redox couple. In contrast, pure PPy exhibited only a sloping curve and a capacity of 20 mAh/g. A three-fold increase in capacity was observed by just anchoring ferrocene onto the PPy backbone. A similar electrosynthesis procedure was utilized here for poly-**9** and resulted in film formation on the current collector. Poly-**9** should exhibit a higher capacity than the PPy/ferrocene composite material due to its higher pendant density (loading) and formation of a dication instead of a cation for the pendant group.

In this chapter, the electrochemical properties of poly-**9** film in various organic electrolyte solutions were first investigated. This was an attempt to determine the optimal device conditions for the polymer film using common organic solvents for electrochemistry. The sample preparation of poly-**9** was achieved by electrodepositing the film directly onto a current collector using the potential step method. The preliminary device testing of the electropolymerized electrode was shown to be very promising. This study validates the concept of a conducting polymer with electroactive pendant groups for future applications in EES.

5-2 Electrochemical Study – Solvent Dependence

Solvent	Dielectric Constant	First Peak, % Lost by 10^{th} Cycle
THF	7.6	10
AN	37.5	40
PC	65	75

Table 5-1. Dielectric constants and percent film deterioration in different solvents.

Tetrahydrofuran (THF), acetonitrile (AN), and propylene carbonate (PC), in order of increasing dielectric constant (Table 5-1), were used to study film electrochemistry.

Lithium-based salts were needed as supporting electrolyte because lithium metal was employed as the anode in the device. Previous electrochemical results did not utilize lithium salts. PC is one of the standard battery solvents, but AN and THF are not practical solvents for lithium-based devices; AN will react with lithium to form methane and lithium cyanide, whereas THF has a high vapor pressure. However, it is assumed that if other solvents with similar dielectric constants are used, the polymer films will behave similarly. Of course, other physical properties such as viscosity can play a major role on electrochemical performance.

To demonstrate the solvent's influence on cyclability, poly-**9** films were first polymerized in AN and subsequently tested in THF, AN, and PC solutions. Using cyclic voltammetry on glassy carbon, poly-**9** films were scanned up to 700mV vs Ag/Ag^+ (4.2V vs Li/Li^+) and cycled ten times in different solvents with 0.1 M lithium perchlorate ($LiClO_4$) as supporting electrolyte (Figure 5-4). In AN and PC, the first faradaic wave is ascribed to the oxidation of the TAPD pendant to its cation and the second wave to the formation of the dication. Upon switching the potential scan, the reductions of the dication and cation are observed, respectively. The films also displayed the typical broad response from PEDOT. The subsequent cycling of the films was significantly influenced by the solvent. The polymer films exhibited the fastest deterioration of the first redox peak in PC with a loss of 75% of its activity by the tenth cycle (Table 5-1). With lower dielectric constant solvents, the ion pairing of the cationic pendant and counter ion is stronger, which may impart greater stability to the pendant. The primary factor in film deterioration is not from the PEDOT backbone, but from the pendant itself since the double-layer capacitance from PEDOT did not significantly change during the

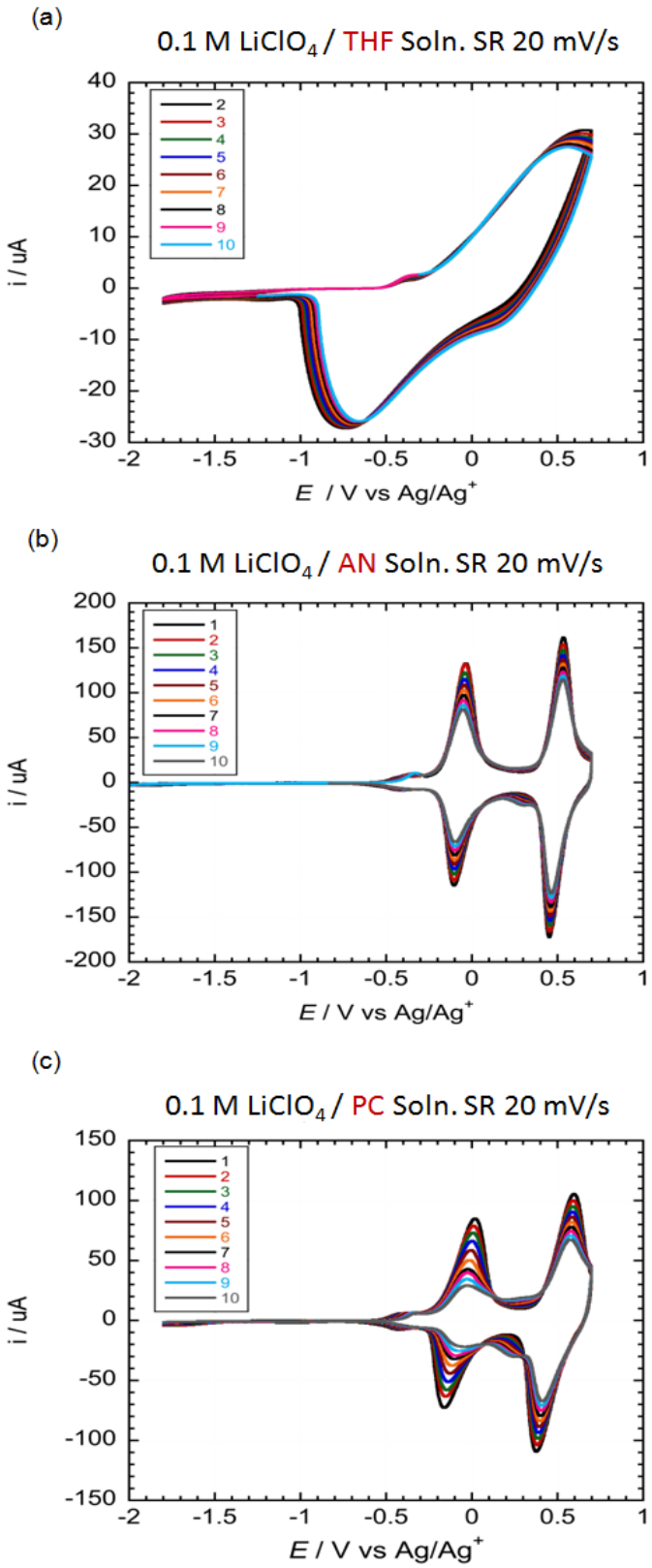

Figure 5-4. Film electrochemistry of poly-**9** in different solvents.

charge/discharge cycling. While in THF, the film exhibited the highest film/solution resistance but afforded the most stable performance at 700mV vs Ag/Ag^+, likely from the greater ion pairing stabilization or that not all charges being accessed (only cation formation). The nucleophilicity of the solvent can play a major role in the stability of the pendant, where the cation would be less reactive (less electrophilic) than the dication towards nucleophiles. Assuming that solvents with both low dielectric constant and low nucleophilicity would likely afford high stability in cycling, tetraglyme (ε_r of 7.70, a common battery solvent) was decided to be the first choice of solvent used for device testing.

5-3 Sample Preparation and Device Testing

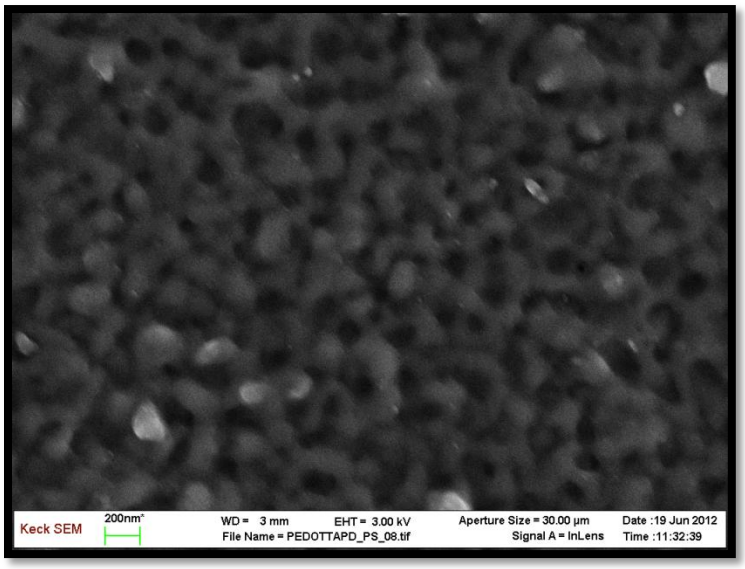

Figure 5-5. SEM image of poly-**9**.

Poly-**9** was electrodeposited onto the current collector by holding the potential at +1.2V vs Ag/Ag^+ for 20 minutes in the monomer containing solution. Film morphology can have a dramatic impact on electrochemical performance. As shown in the SEM image in Figure 5-5, depositing poly-**9** using potential step yields a porous (less-dense)

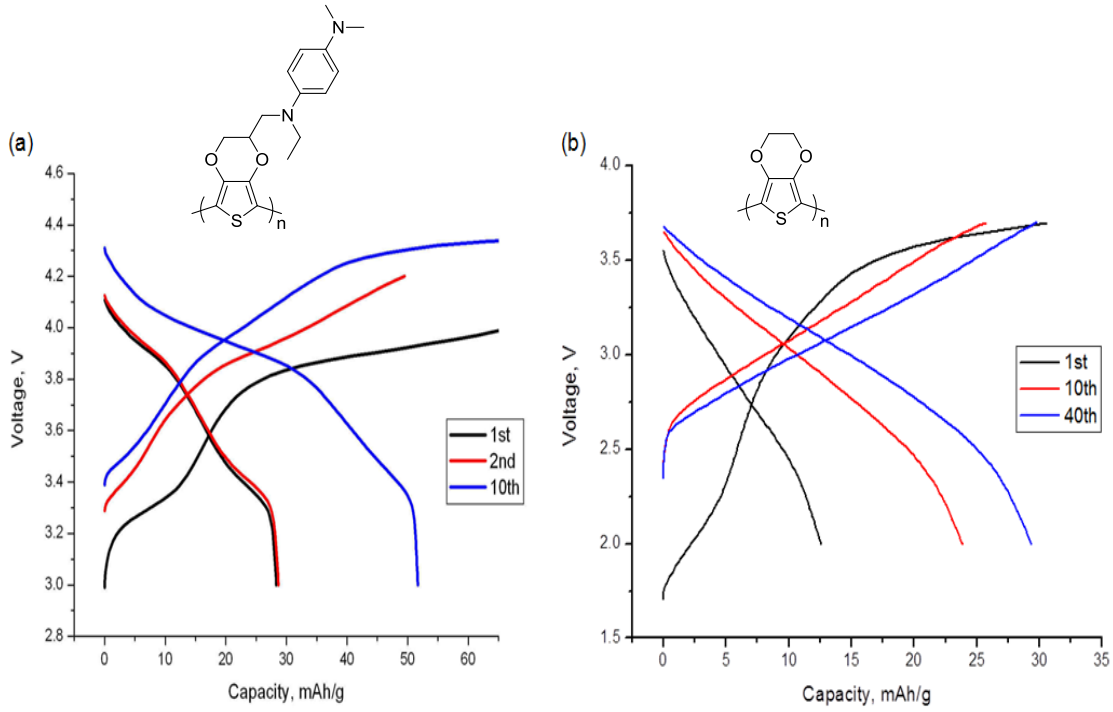

Figure 5-6. Charge-discharge curves of (a) poly-**9** and (b) PEDOT at 1C.

polymer film. Having a porous film would be advantageous due to higher ion (electrolyte) mobility and accessibility, which in turn, would lead to higher power capability (smaller overpotential).

The preliminary device testing of the electropolymerized electrode (Figure 5-6) is very promising as evidenced by the high voltage and increased capacity over traditional conducting polymers, all the while negating the need for conducting additives and binders. The device was composed of poly-**9** as a cathode, lithium metal as an anode, and 1M lithium bis(trifluoromethane)sulfonimidate (LiTFSI) in tetraglyme as the electrolyte. The cells were galvanostatically charged and discharged with a current density of 50 mA/g (corresponding to ~1C) between 3 to 4.2V vs Li/Li^+. In the charging process, both TAPD and PEDOT segments are oxidized and TFSI counter anions diffuse into the film from the electrolyte solution to maintain charge neutrality. During

discharge, the oxidized film is reduced back to its neutral form and the TFSI anions return to solution. Poly-**9** film exhibited capacities of up to 53 mAh/g during discharge with two voltage plateaus near 3.9 and 3.5 V corresponding to the two faradaic redox processes from the TAPD pendant. The sloping downward component of the discharge curve arises from the pseudocapacitance of PEDOT (Figure 1-1 for capacitor). By comparing the 10^{th} discharge curves of Figure 5-6 (a) and (b), the capacity of poly-**9** is approximately twice that of a pure PEDOT film (25mAh/g). However, the film exhibits a significant overcharge and only one fourth of its theoretical capacity. One possibility is that tetraglyme behaves similarly to THF. The low capacity may also be attributed to the degradation of the pendant groups during film preparation. The prolonged oxidizing environment gives enough time for the dication to react with the solvent or any traces of water. Potential cycling method should be looked at in the future for less straining condition it provides (able to cycle back before side-reactions occur) during deposition and better film morphology from its slower polymer growth. Nevertheless, this initial investigation of poly-**9** demonstrated the promise of this 'hybrid' approach for conducting polymers in EES applications.

5-4 Summary & Conclusions

A 'hybrid' conducting polymer has been studied as an electrode material for EES applications and demonstrated the enhancement of capacity through the immobilization of electroactive organics onto a conducting polymer. When cycled in AN and PC, poly-**9** exhibited two well-defined faradaic processes due to the redox reactions of TAPD in addition to the current response from PEDOT backbone. The solvent greatly influenced the stability of the film during the charge/discharge cycles. Initially, oxidative chemical

polymerization was attempted multiple times with different reagents to form poly-**9** for device testing, but unsuccessful results followed. Instead, electrosynthesis was utilized to deposit a porous poly-**9** film onto the current collector using the potential step method. The early device testing of poly-**9** exhibited capacities up to 53 mAh/g, approximately twice that of a pure PEDOT film. While further improvement of the cycling performance is necessary before use in practical applications, this preliminary work demonstrates a feasible methodology to prepare organic electrode materials coupled with superior energy densities for EES. Next, designing and fabricating novel nano-architectures, such as an array of nanorods for poly-**9,** will further enhance its performance and its power capability.

5-5 Comments on 'Hybrid' Materials

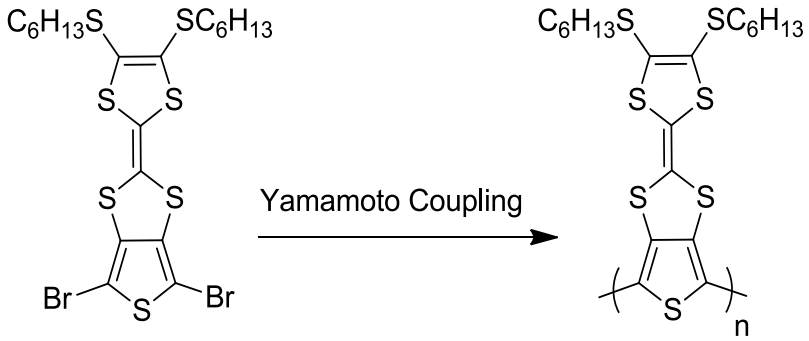

Figure 5-7. Polymerization of Thiophene-Tetrathiafulvalene monomer utilizing Yamamoto coupling.

Although directly depositing 'hybrid' polymers onto current collector is convenient, the potential degradation of the pendant during the preparation is concerning. As previously mentioned, instead of the potential step, potential cycling may provide a less-degraded polymer film from shorter oxidizing environment it experiences (sweep back before any side-reactions occurs). The optimal choice is to employ a non-oxidative

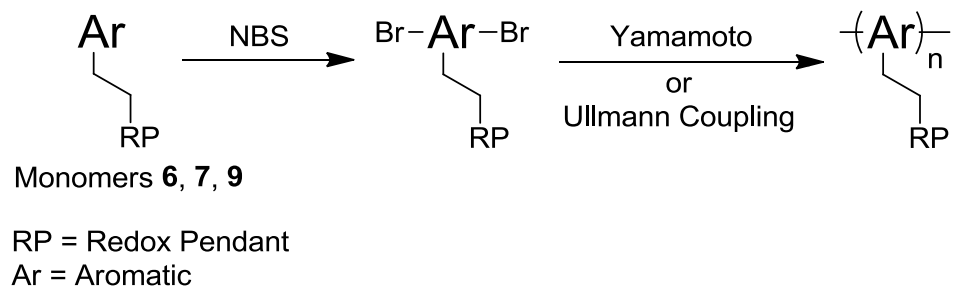

Figure 5-8. New synthesis scheme for TAPD 'hybrid' polymers.

polymerization to prevent any possible pendant degradation. Skabara et al. has successfully demonstrated a non-oxidative method to couple 'hybrid' monomeric species by producing poly-(Thiophene-Tetrathiafulvalene), a 'hybrid' polymer (Figure 5-7) utilizing Yamamoto coupling.[6] The electrochemistry of poly-(Th-TTF) gives two reversible faradaic waves (two electrons per monomer unit) consistent with the two redox couples of TTF. One important message delivered from the authors is the complications of electropolymerizing polymer backbones with redox-active pendant groups as observed in the case of TAPD 'hybrid' materials using pyrrole as the electropolymerizable unit. With a non-oxidative method, it is possible to polymerize monomers **6** and **7**, producing polymeric materials with higher energy densities and higher capacities than the PEDOT-based 'hybrids' as a result of the decreased mass. Figure 5-8 depicts a new chemical synthesis scheme of TAPD 'hybrid' polymers that starts from already synthesized monomers. The first step of bromination using NBS has already been demonstrated either in the literature[7] or in the works of the Abruña group. By utilizing Yamamoto (similar to poly-(Th-TTF)) or Ullmann coupling, the final polymer product of interest will be obtained. There is an urgent need to optimize the electrosynthesis and the non-oxidative polymerization to further advance this type of material. In addition to this,

truly understanding the fundamental degradation pathways during charge/discharge cycling will also help significantly improve cycling performances. One method that comes to mind is electrochemical techniques coupled to RAMAN spectroscopy.

5-6 References

1. A. Ito, D. Sakamaki, H. Ino, A. Taniguchi, Y. Hirao, K. Tanaka, K. Kanemoto and T. Kato, *Eur. J. Org. Chem.*, 2009, **26**, 4441.
2. M. Morimoto, S. Kobatake and M. Irie, *Chem. Commun.*, 2006, **25**, 2656.
3. L. Michaelis, M. P. Schubert and S. Granick, *J. Am. Chem. Soc.*, 1939, **61**, 1981.
4. M. Aydin, B. Esat, C. Kilic, M. E. Kose, A. Ata and F. Yilmaz, *Eur. Polym. J.*, 2011, **47**, 2283.
5. K.-S. Park, S. B. Schougaard and J. B. Goodenough, *Adv. Mater.*, 2007, **19**, 848.
6. P. J. Skabara, R. Berridge, E. J. L. McInnes, D. P. West, S. J. Coles, M. B. Hursthouse and K. Mullen, *J. Mater. Chem.*, 2004, **14**, 1964.
7. A. Hildebrandt and H. Lang, *Dalton Trans.*, 2011, **40**, 11831.

CHAPTER SIX

POST-POLYMERIZATION MODIFICATION AS A METHOD FOR GENERATING ELECTROACTIVE HYBRID-POLYMER

6-1 Introduction

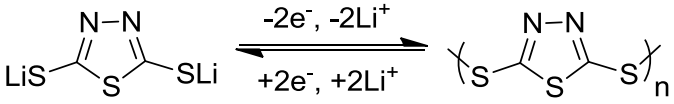

Figure 6-1. Redox property of 2,5-dimercapto-1,3,4-thiadiazole (DMcT).

Organic disulfide compounds are favorable cathode materials for lithium-ion batteries (LIB) due to the organics being readily synthesized out of inexpensive materials and capability to tune, using well-demonstrated principles of organic chemistry.[1-4] Among many, 2,5-dimercapto-1,3,4-thiadiazole (DMcT, Figure 6-1) is noteworthy because of its high theoretical gravimetric capacity (362 mAh/g) and excellent chemical reversibility.[5,6] However, DMcT, like most other small organics, is also soluble in common battery electrolyte media, resulting in poor cyclability for composite electrodes.[7,8] While the initial disulfide polymers are insoluble in organic solvent, the small and highly charged reduced bisthiolate monomers are soluble in the polar media employed in LIBs; ensuring the necessity that these active species remain in contact with the electrode.

Similar to the previous chapters, a 'hybrid' approach will be utilized here, where DMcT is confined onto poly(3,4-ethylenedioxythiophene) (PEDOT) backbone. PEDOT was employed as the substrate instead of other conducting polymers because the sluggish charge transfer kinetics of DMcT are dramatically accelerated by PEDOT, increasing the

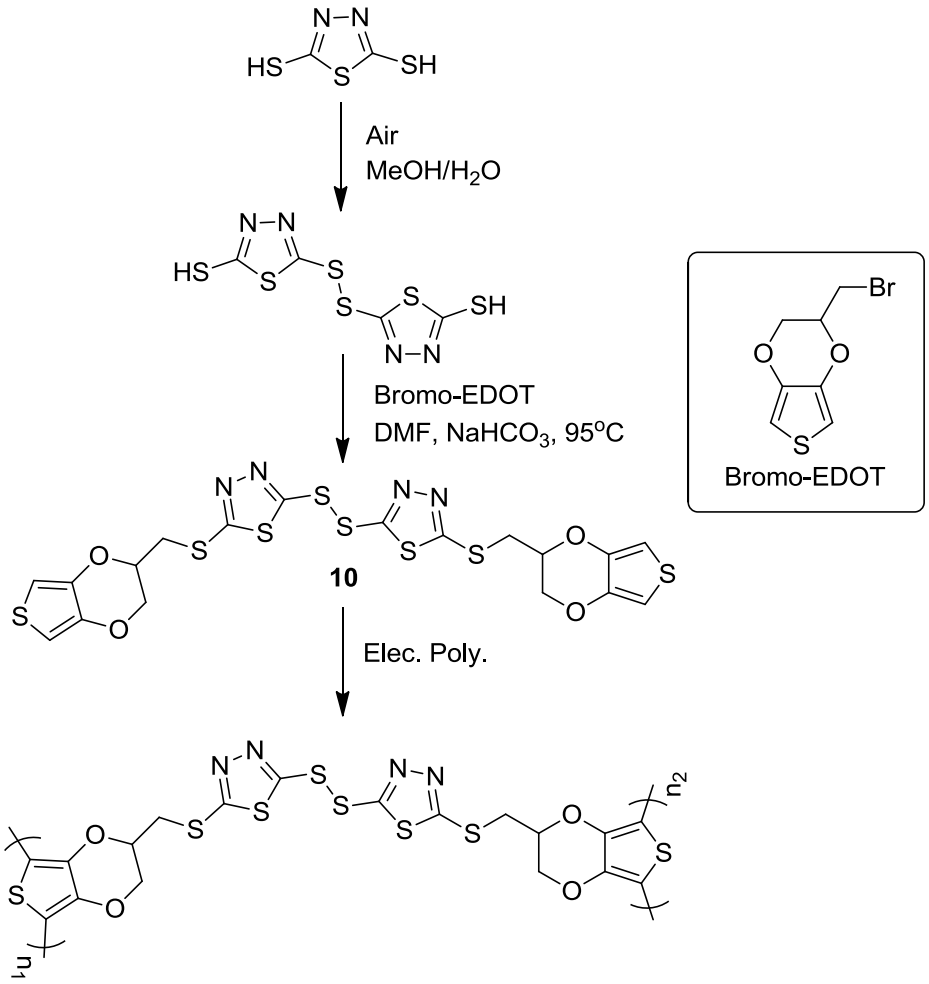

Scheme 6-1. Synthesis scheme of **10** and its electropolymerization.

power density of the cathode.[9-11] PEDOT exhibits excellent chemical stability, a wide window of high conductivity, and capacity (0.6 electron per monomer unit).[12-14] A dimer EDOT-DMcT **10** (Scheme 6-1) was synthesized instead of the free thiol form of EDOT-DMcT to minimize complications that may arise from potential thiolene-type reactions during electropolymerization. After the electropolymerization of **10** on a glassy carbon electrode, the resulting film exhibited a conducting polymer film with a smaller window of conductivity, compared to PEDOT, along with the absence of DMcT's disulfide-thiolate redox couple. With no success for this approach, a different method was required.

This chapter outlines a methodology in attaching DMcT molecules directly to a PEDOT backbone using a post-polymerization modification method. The feasibility of this approach has been demonstrated in the literature (i.e. anchoring of tetrathiafulvalene (TTF) onto PEDOT).[15] While the poly-(EDOT-DMcT) hybrid material has a lower theoretical capacity than pure DMcT, due to the loss of one thiolate as a point of attachment to the polymer backbone, this material has a theoretical capacity of 141mAh/g, comparable to traditional inorganic battery electrodes like $LiCoO_2$ and $LiFePO_4$.

6-2 Synthesis of Poly-(EDOT-DMcT)

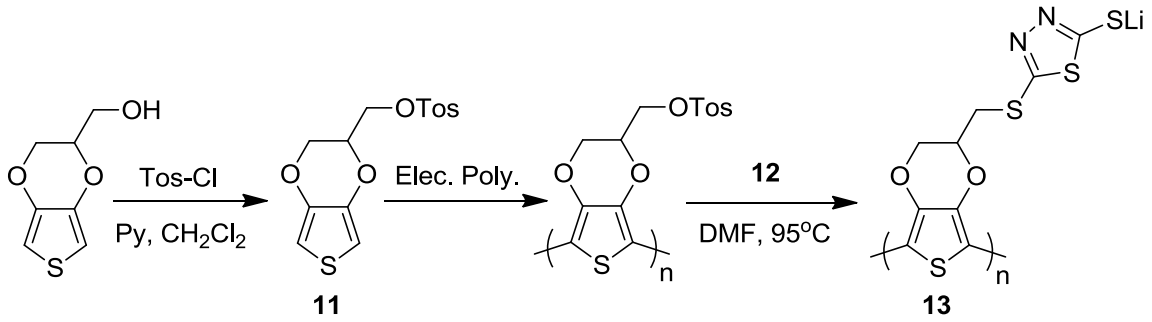

Scheme 6-2. Synthesis scheme of 'hybrid' polymer **13**.

Scheme 6-2 depicts the synthetic route for poly-(EDOT-DMcT) **13**. An EDOT monomer with a pendant tosylate group (EDOT-OTs **11**) was incorporated by tosylating hydroxymethyl-EDOT. Monomer **11** was subsequently electropolymerized on a glassy carbon electrode. The resulting polymer film displayed cyclic voltammetric responses nearly identical to those of a typical PEDOT film (Figure 6-2), indicating the bulky tosylate group does not alter the electronic properties of PEDOT. The electrochemically-generated films were then exposed to a 0.5 M solution of dilithiated DMcT **12**[16] in *N*,*N*-dimethylformamide at 95ºC. The reaction progress was monitored via cyclic voltammetry

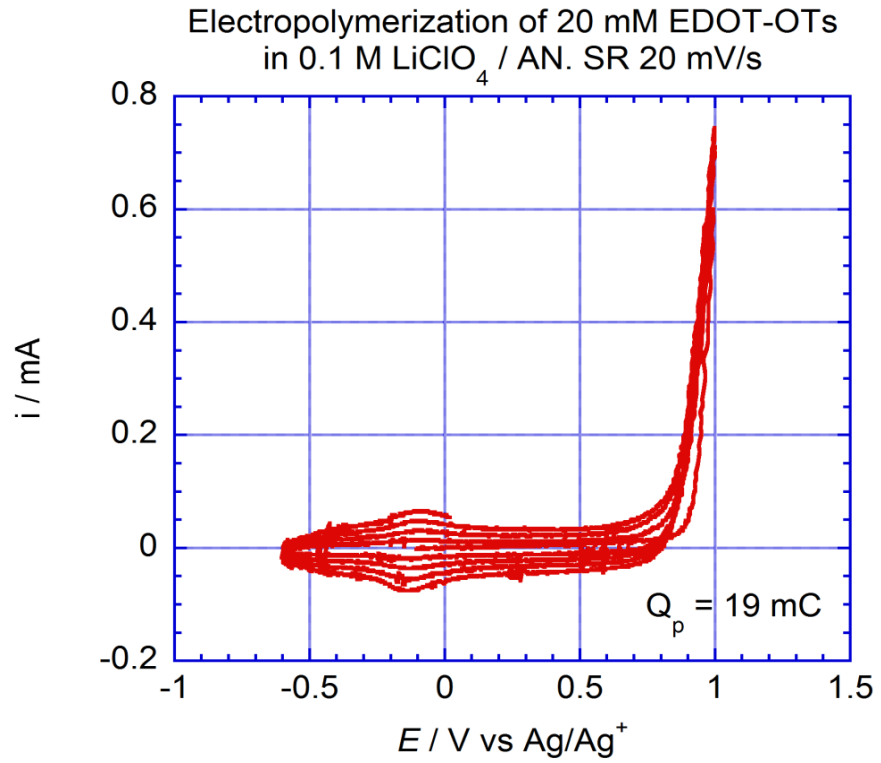

Figure 6-2. Electropolymerization of EDOT-OTs **11**.

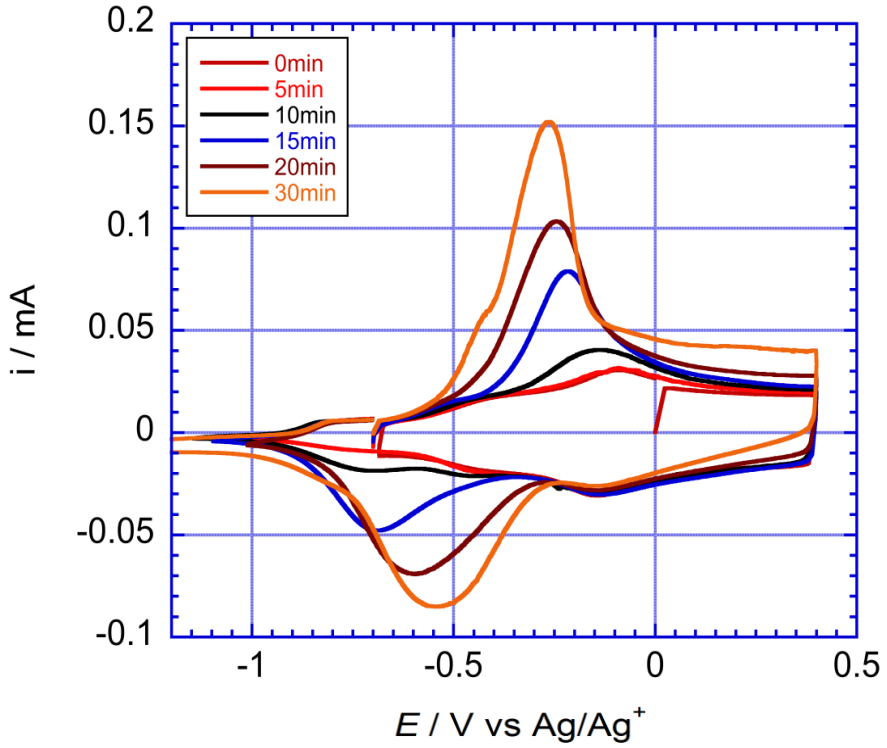

Figure 6-3. Reaction progress of **11** with dilithiated DMcT **12**.

(CV) with the modified electrode placed in a DMcT-free solution in specific time interval until no further indication of incorporated DMcT was present (Figure 6-3). During the modification, the peak current of the redox couple of DMcT increased as time progressed until stabilizing after thirty minutes. The electrode was subsequently washed with acetone and acetonitrile.

6-3 Electrochemical Characterization & Cyclability

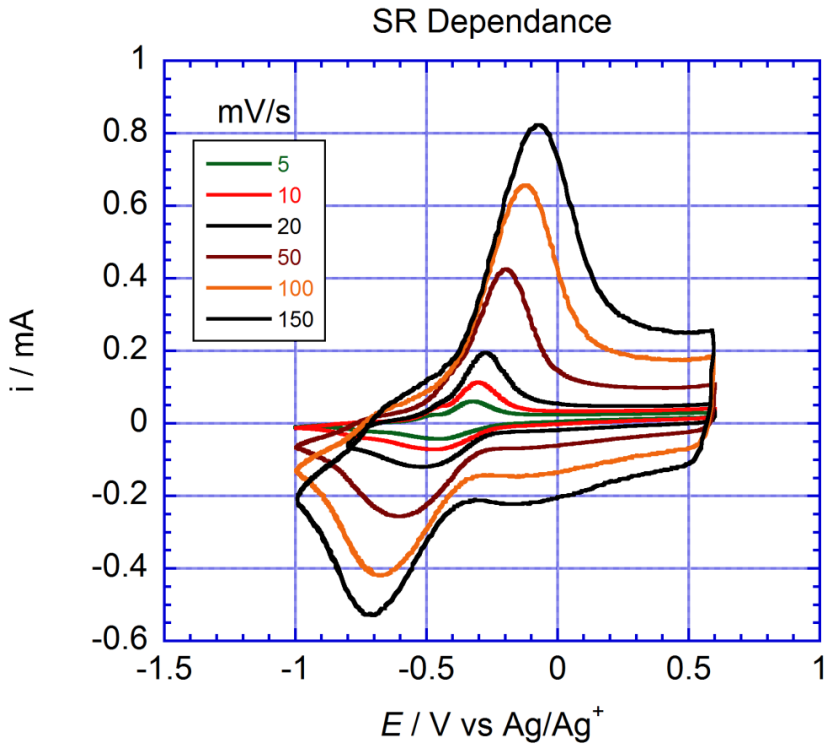

Figure 6-4. Scan rate dependence of **13**.

As shown in Figure 6-4, the CV of the new 'hybrid' polymer poly-(EDOT-DMcT) **13** displayed a redox response at approximately -0.40 vs. Ag/Ag^{+}, corresponding to the disulfide-thiolate redox couple of DMcT. The chemical modification and bulky DMcT group on the PEDOT backbone did not change the pseudocapacitance or window of conductivity of PEDOT. The DMcT peak separation for **13** is smaller than DMcT for a bare glassy carbon electrode. The 'hybrid' material retains both charge storage and

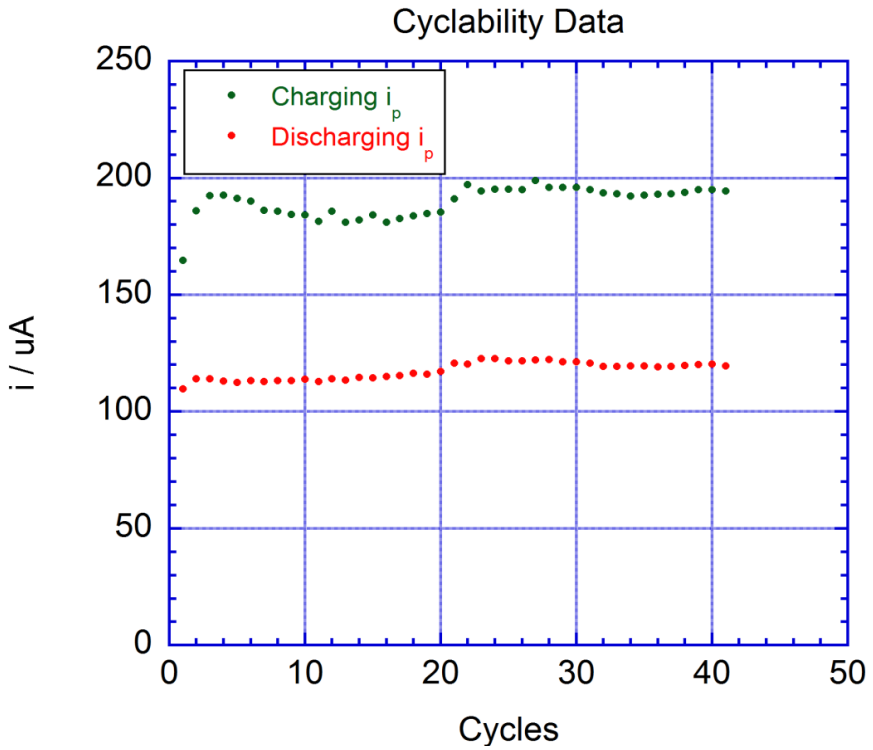

Figure 6-5. Cyclability performance of **13**.

electrocatalyst capabilities. Though the peak to peak separation is larger than DMcT at a PEDOT modified electrode, the value decreased significantly at very low scan rates. Ionic motion may explain the difference in peak shape for the oxidation and reduction processes. At high scan rates, the reaction is limited by diffusion of lithium ions through the polymer film. The repulsion between the lithium ions and the positively-charged polymer may facilitate lithium ion transfer out of the film, arising in a sharper current peak in the oxidation process than the reduction.

Depicted in Figure 6-5, the hybrid material showed almost no deterioration over forty cycles while cycling at a rate of 20 mV/s. It must be emphasized that this is an extremely fast charge/discharge rate (approximately 120C with full charge in 30s).

6-4 Summary & Conclusions

By preparing a hybrid material that incorporates both the PEDOT electrocatalyst in the polymer backbone and a pendant disulfide moiety for charge storage, it was possible to obtain both high rate performance and high capacity. PEDOT serves multiple functions, not only as an electrocatalyst, but also as a conducting film, anion reservoir, and insoluble anchor for DMcT molecules. While **13** has a lower theoretical capacity than pure DMcT (partly compensated by the 0.6 electron from PEDOT), it has demonstrated the strengths of confining the charge storage material to the electrode surface via a polymer electrocatalyst. This preliminary result is a promising demonstration of capacity retention in an organic material with high-rate capability. In order to incorporate this material into a device, either chemically or electrochemically EDOT-OTs **11** has to be polymerized onto a current collector directly and then applying the same reaction condition previously used for post-polymerization.

6-5 References

1. S. J. Visco, C. C. Mailhe, L. C. De Jonghe and M. B. Armand, *J. Electrochem. Soc.*, 1989, **136**, 661.
2. Y. Liang, Z. Tao and J. Chen, *Adv. Energy Mater.*, 2012, **2**, 742.
3. J. Gao, M. A. Lowe, S. Conte, S. E. Burkhardt and H. D. Abruña, *Chem. Eur. J.*, 2012, **18**, 8521.
4. H. D. Abruña, F. Matsumoto, J. L. Cohen, J. Jin, C. Roychowdhury, M. Prochaska, R. B. van Dover, F. J. DiSalvo, Y. Kiya, J. C. Henderson and G. R. Hutchison, *Bull. Chem. Soc. Jpn.*, 2007, **80**, 1843.
5. Y. Kiya, J. C. Henderson, G. R. Hutchison and H. D. Abruña, *J. Mater. Chem.*, 2007, **17**, 4366.

6. K. Naoi, K. Kawase and Y. Inoue, *J. Electrochem. Soc.*, 1997, **144**, L170.

7. X. Yu, J. Xie, J. Yang, H. Huang, K. Wang and Z. Wen, *J. Electroanal. Chem.*, 2004, **573**, 121.

8. T. Chi, H. Li, X. Li, H. Bao and G. Wang, *Electrochim. Acta*, 2013, **96**, 206.

9. N. Oyama, Y. Kiya, O. Hatozaki, S. Morioka and H. D. Abruña, *Electrochem. Solid St.*, 2003, **6**, A286.

10. Y. Kiya, O. Hatozaki, N. Oyama and H. D. Abruña, *J. Phys. Chem. C*, 2007, **111**, 13129.

11. G. G. Rodriguez-Calero, M. A. Lowe, Y. Kiya and H. D. Abruña, *J. Phys. Chem. C*, 2010, **114**, 6169.

12. J. C. Carlberg and O. Inganas, *J. Electrochem. Soc.*, 1997, **144**, L61.

13. X. Cui and D. C. Martin, *Sensor Actuat. B-Chem.*, 2003, **89**, 92.

14. F. Estrany, D. Aradilla, R. Oliver and C. Aleman, *Eur. Polym. J.*, 2007, **43**, 1876.

15. M. Balog, H. Rayah, F. Le Derf and M. Salle, *New J. Chem.*, 2008, **32**, 1183.

16. J. M. Pope, T. Sato, E. Shoji, D. A. Buttry, T. Sotomura and N. Oyama, *J. Power Sources*, 1997, **68**, 739.

CHAPTER SEVEN

FUTURE DIRECTIONS

7-1 Future Research Directions

The emergent need to find successful electrical energy storage (EES) systems naturally led to the examination of organic materials. The plenitude of resources for organic compounds offers the additional benefits of decreased cost and abundancy as compared to metal oxides and phosphates. Furthermore, their chemical tunability reinforces these materials to be even more attractive by enabling fine tuning of properties such as charge transfer kinetics (power capability) and redox potentials (voltage).

This dissertation focused on the organic synthesis and electrochemical characterization of new redox-active organic materials for next generation high-energy cathode materials for EES devices. While the work presented in the previous chapters sets a firm foundation for future materials, there is still more research and optimization that need to be accomplished as listed below:

1) Search for greater capacity/energy and more stable electroactive materials.
2) Optimize electrosynthesis of 'hybrid' polymers and device testing condition.
3) Employ a non-oxidative polymerization process for producing 'hybrid' polymers to eliminate any potential degradation of the pendant groups.
4) Implementation of post-polymerization modification method at the device level.

7-2 Electropolymerization of Non-Conductive Redox Polymers

The electropolymerization method established for 'hybrid' polymers can be

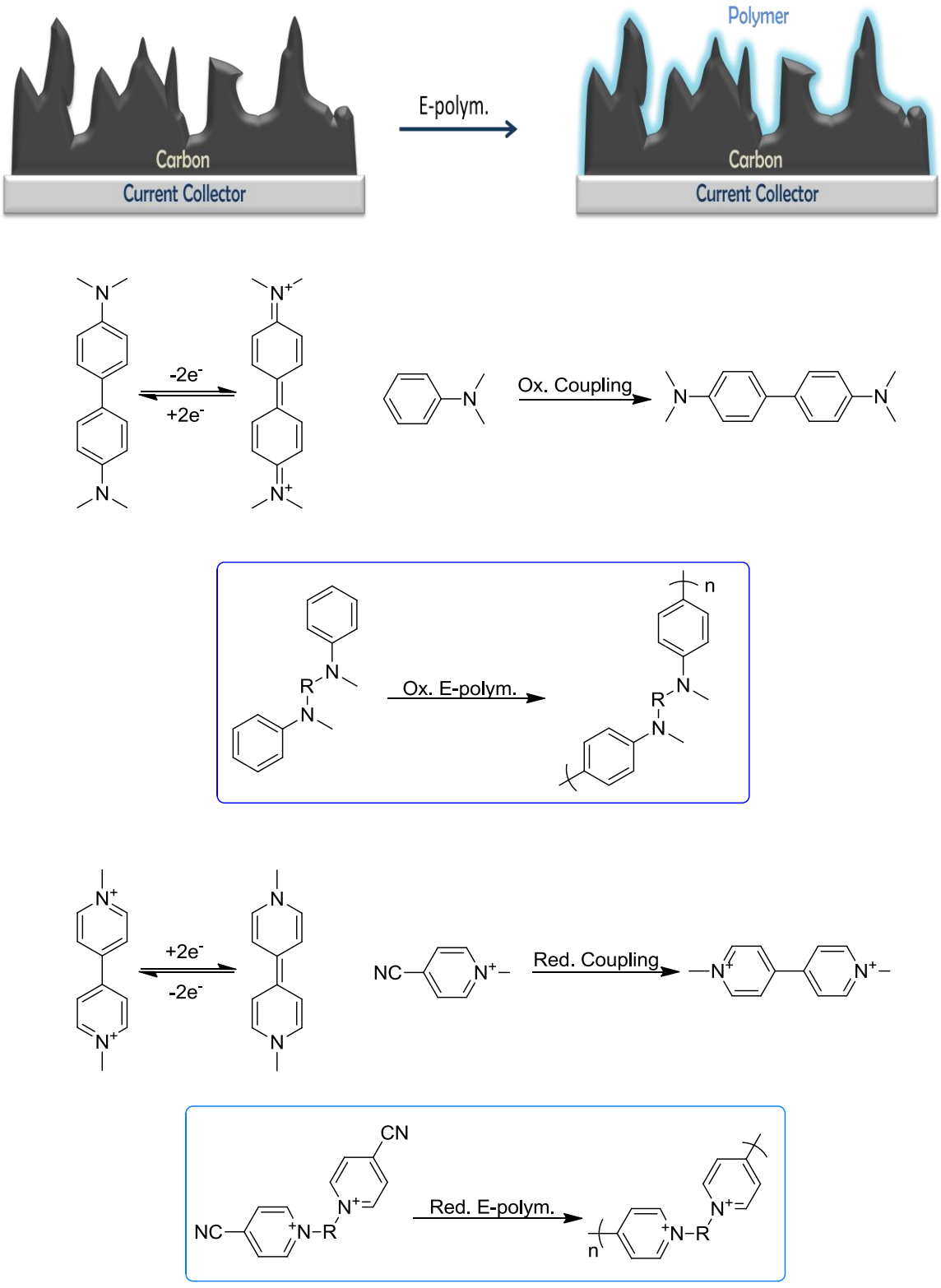

Figure 7-1. Electropolymerization of non-conductive redox polymers on carbon.

employed in depositing non-conducting redox-active polymers onto carbon-coated current collector (Figure 7-1). With the knowledge of oxidative coupling of *N*,*N*-dimethylaniline or reductive coupling of 4-cyano-1-methylpyridinium salt, it is possible to form polymers of redox-active units respectively as N,N,N',N'-tetramethylbenzidine or viologens along the polymer backbone.[1,2]

7-3 Symmetric EES Devices

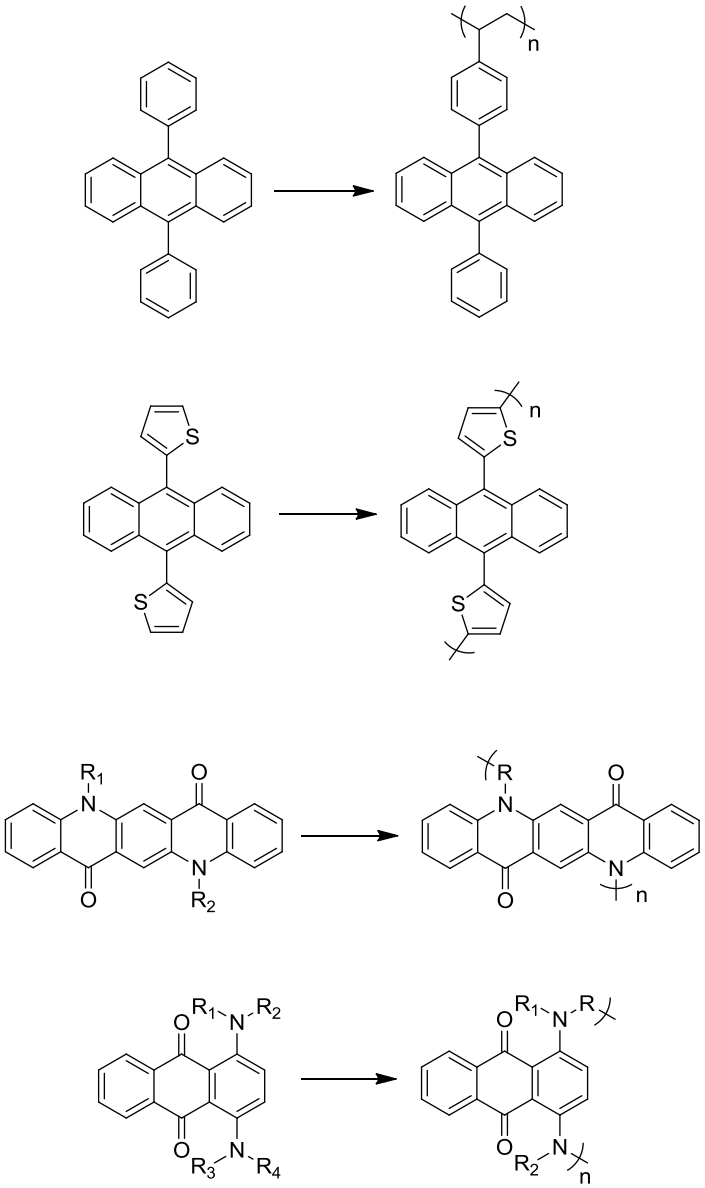

Figure 7-2. Symmetric EES electrode monomers and its polymeric form.

ECL-based (electrochemiluminescence) compounds are another class of materials that are noteworthy for EES applications because of their bipolaron behavior, allowing these materials to be employed as symmetric electrodes in EES devices (i.e., 9,10-diphenylanthracene can give stable cations and anions). Again, due to high solubility of organics in electrolyte media, these compounds must be confined to a polymeric backbone. Figure 7-2 depicts several ECL monomeric species and their polymeric form. The thiophene-substituted 9,10-diphenylanthracene is promising as its deposition can be directly performed on a current collector using electrosynthesis. The only concern of this material is that it may act similarly to a conducting polymer instead of behaving like a bipolaron. The last two molecules in Figure 7-2 use TAPD and carbonyl functionalities to obtain oxidative and reductive capabilities. These compounds will offer great capacities due to the capability of providing two oxidations and two reductions.

7-4 Anchoring Electroactive Compounds on Other Insoluble Substrates

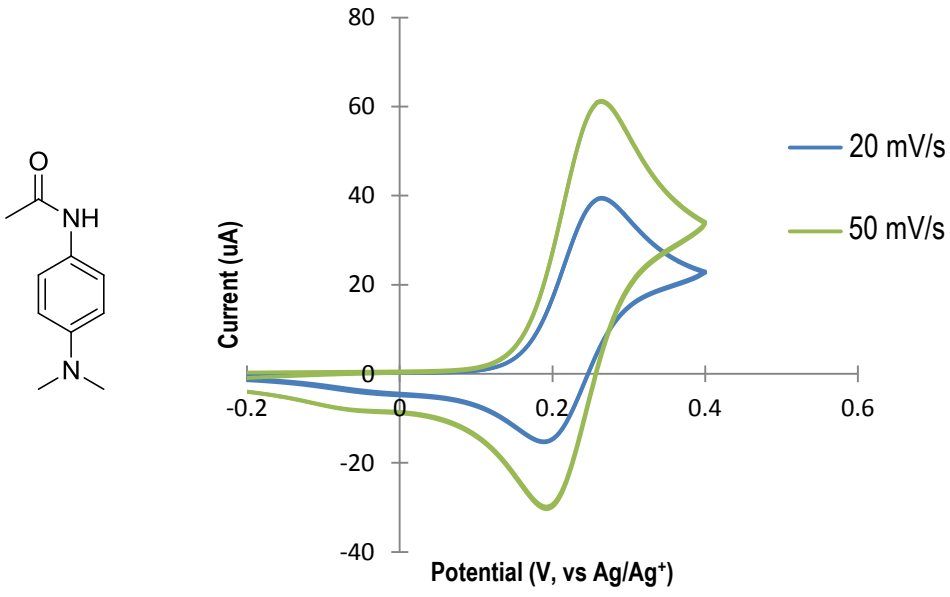

Figure 7-3. CV of 3mM of acetyl-DMPD in 0.1M TBAP/AN.

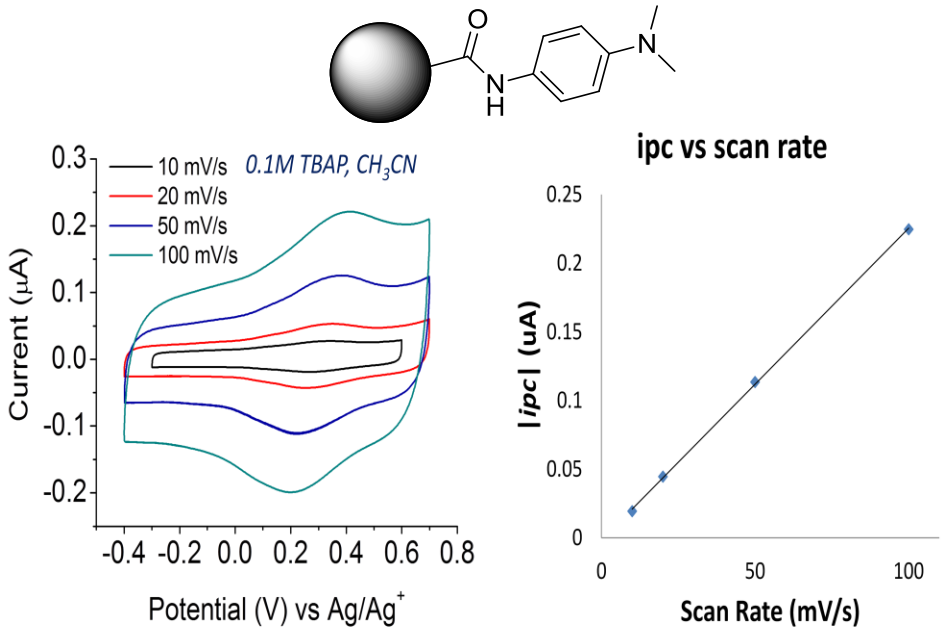

Figure 7-4. CV of DMPD-carbon composite and the plot of i_{pc} vs scan rate.

Instead of using conducting polymeric backbone, it would be appealing to anchor electroactive compounds onto another insoluble substrate, namely carbon. There are many types of grafting procedures available in literature. Figure 7-3 depicts the reversible electrochemistry of acetylized *N*,*N*-dimethyl-*p*-phenylenediamine (acetyl-DMPD). With the knowledge of acetyl-DMPD affording reversible redox couple, carboxyl groups on carbon were utilized to connect DMPD through amide linkage. The DMPD-carbon composite displays a redox response corresponding to the acetyl-DMPD (Figure 7-4). The disadvantage of this approach is that the loading of redox-active molecules is lower compared to polymeric 'hybrid' approach. Therefore, loading of these compounds onto carbon must be optimized utilizing different grafting methodologies, grafting conditions, and types of carbons.

7-5 References

1. R. Hand and R. F. Nelson, *J. Electrochem. Soc.*, 1970, **117**, 1353.

2. T. Saika, T. Iyoda and T. Shimidzu, *Bull. Chem. Soc. Jpn.*, 1993, **66**, 2054.